EFFECTS OF CONTACTOR SIZE AND STIMULATION DISTANCE ON THE RESPONSE PROPERTIES OF RAPIDLY-ADAPTING TACTILE FIBERS INNERVATING THE RAT GLABROUS SKIN

by

İsmail Devecioğlu

B.S., Electronics and Communication Teaching, Marmara University, 2009

Submitted to the Institute of Biomedical Engineering
in partial fulfillment of the requirements
for the degree of
Master of Science
in
Biomedical Engineering

Boğaziçi University
2011

EFFECTS OF CONTACTOR SIZE AND STIMULATION DISTANCE ON THE RESPONSE PROPERTIES OF RAPIDLY-ADAPTING TACTILE FIBERS INNERVATING THE RAT GLABROUS SKIN

APPROVED BY:

Assoc. Prof. Dr. Burak Güçlü .....
(Thesis Advisor)

Prof. Dr. Ahmet Ademoğlu .....

Prof. Dr. Reşit Canbeyli .....

DATE OF APPROVAL: 26 August 2011

ACKNOWLEDGMENTS

I'm grateful to my family for their support and encouragement during my master study.

I specially thank to my advisor Burak Güçlü for his support, help and motivation during all stages of the thesis.

I thank to Prof. Dr. Reşit Canbeyli and Prof. Dr. Ahmet Ademoğlu for their precious comments, and Mustafa Zahid Yıldız, Daniel Press and Murat Özsaltik for their help and comments.

I also thank to Namık Kemal Univesity Biomedical Engineering Department for their motivational support and to Mechanical Engineer İbrahim Mutlu and Technician Erhan Kuşçu for their technical support.

ABSTRACT

EFFECTS OF CONTACTOR SIZE AND STIMULATION DISTANCE ON THE RESPONSE PROPERTIES OF RAPIDLY-ADAPTING TACTILE FIBERS INNERVATING THE RAT GLABROUS SKIN

Recent population models used space-invariant attenuation functions. But this assumption is not enough to construct realistic population models, because mechanical properties of the skin vary along the skin [1]. In this study, it is hypothesized that response profiles of mechanoreceptive fibers are not symmetric along proximo-distal axis due to the varying mechanical properties of the skin.

In this study, sinusoidal mechanical vibrations were applied perpendicular to the skin of adult rats. Single-unit responses were recorded from sciatic nerve. Five different stimulus locations (2 distal, 1 RF center, 2 proximal) and three different contactor sizes (area: 0.39 mm^2, 1.63 mm^2, 2.96 mm^2) were used. Averages of absolute spike thresholds (a_0) and entrainment thresholds (a_1) of rapidly adapting fibers were plotted as a function of stimulation distance and contactor size. Also, mechanical impedance of the skin was measured at 5 different locations on distal phalanx of one rat.

2-way ANOVA showed that the effect of stimulus location on a_0 and a_1 was significant ($p<0.001$), whereas contactor size had no significant effects ($p=0.642$). Post-hoc Tukey test showed that thresholds for proximal stimulations were higher than those for distal stimulations. A mechanical model which explains the mechanical behavior of the skin and its effects on mechanoreceptive fibers' response is presented.

According to these results rate-intensity functions of RA fibers shift asymmetrically along the proximo-distal axis, which suggests that the mechanical stimulus is transmitted better towards the proximal direction. This may counterbalance the effects of innervation density and cause uniform psychophysical detection thresholds for the finger.

Keywords: Somatosensation, tactile fiber, vibrotactile stimulus, skin mechanics.

ÖZET

UYARIM UCU BÜYÜKLÜĞÜ VE UYARIM UZAKLIĞININ SIÇAN TÜYSÜZ DERİSİNDEKİ ÇABUK ALIŞAN DOKUNMA SİNİRLERİNİN CEVABINA ETKİSİ

Mevcut mekanoreseptör kitle modelleri mekandan bağımsız zayıflama fonksiyonları kullanmaktadır. Ancak bu varsayım gerçekçi kitle modelleri oluşturmak için yeterli değildir, çünkü derinin mekanik özellikleri deri boyunca farklılık göstermektedir [1]. Sunulan çalışmada, derinin mekanik özelliklerinin değişiklik göstermesinden dolayı mekanoreseptörlerin cevap profillerinin proksimo-distal eksende simetrik olmadığı hipotez edilmiştir.

Sunulan çalışmada, sinüzoidal mekanik titreşimler yetişkin sıçanların derisine dik bir şekilde uygulanmış ve siyatik sinirden tekil aksiyon potansiyeli kayıtları gerçekleştirilmiştir. 5 farklı uyarım uzaklığı (2 distal, 1 duyar alan merkezi, 2 proksimal) ve üç farklı uyarım alanı büyüklüğü (alan: 0.39 mm^2, 1.63 mm^2, 2.96 mm^2) kullanılmıştır. Çabuk alışan mekanoreseptörlere ait ortalama mutlak aksiyon potansiyeli eşiği (a_0) ve senkron atım eşiği (a_1) değerleri uyarım alanı ve uyarım uzaklığına karşı grafik olarak çizilmiştir. Ayrıca bir sıçanın parmak ucunda derinin mekanik empedansı 5 farklı noktada ölçülmüştür.

2-way ANOVA sonuçlarına göre uyarım uzaklığının a_0 ve a_1 değerlerini istatistiksel anlamda etkilediği görülmektedir ($p<0.001$), fakat uyarım alanı büyüklüğünün istatistiksel anlamda bir etkisi görülmemektedir ($p=0.642$). Post-hoc Tukey testi proksimal uyarımlardaki eşik değerlerinin distal uyarımlardaki eşik değerlerinden yüksek olduğunu göstermiştir. Derinin mekanik davranışını ve mekanoreseptör cevabı üzerindeki etkisini açıklayan bir deri mekanik modeli sunulmuştur.

Uyarım-yanıt fonksiyonlarının proksimo-distal eksendeki asimetrisi mekanik uyarımın bir yöne doğru daha iyi iletildiğini göstermektedir. Bu durumun sinir yoğunluğu etkilerini dengelerken parmakta sabit bir pisikofiziksel algılama eşiği yarattığı düşünülmektedir.

Anahtar Sözcükler: Beden duyusu, dokunma siniri, titreşimsel uyarım, deri mekaniği.

TABLE OF CONTENTS

LIST OF FIGURES

LIST OF TABLES

LIST OF SYMBOLS

a_0	Absolute spike threshold
a_1	Entrainment threshold
Z	Mechanical impedance
F	Force
x	Displacement
v	Velocity
b	Damper constant (resistance)
k	Spring constant (stiffness)
m	Mass
i, j	Imaginary unit
t	Time
w	Angular velocity
P	Proximal
D	Distal
d	Distance
s	Static indentation
ϕ	Phase angle between the force and the velocity
Δ	Displacement in springs

LIST OF ABBREVIATIONS

SAI	Slowly adapting type I affrent
SAII	Slowly adapting type II afferent
RA	Rapidly adapting afferent (for human; FAI)
PC	Pacinian afferent (for human; FAII)
RF	Receptive field
MCN	Merkel cell-neurite complex
AP	Action potential
CNS	Central nervous system
ECM	Extracellular matrix
SNR	Signal to noise ratio
IP	Intraperitoneal
SE	Standard Error
NP	Non-Pacinian channel
FNS	Functional neuromuscular stimulation

1. INTRODUCTION

1.1 Motivation

Tactile information resulting from peripheral mechanoreceptive fibers is important in order to explore our environment and to interact with it. It also has roles during our motor activity; for example, information send by tactile afferents are used during gripping an object in order to adjust gripping force. However, tactile information and motor activity are disabled in many spinal traumas. Recent studies [2, 3, 4, 5, 6, 7, 8, 9] involve design and improvement of neuroprosthesis and functional neuromuscular stimulation (FNS) systems to restore motor activity of people who are devoid of touch sensation and muscle movement. FNS systems involve controlled stimulation of muscles dependent on many different input systems such as foot drop switches or pressure sensors or electroneurogram (ENG) signals. However, non of these systems provide the recovery of touch sense. London et al. (2008) and Romo et al. (1998) showed that it is possible to emulate the tactile senses on periphery by stimulating the somatosensory cortex. The best solution for FNS systems might be to use peripheral population response data as tactile feedback. This can be achieved by a mechanical transducer which may produce electrical signals that represent a population of mechanoreceptive fibers. For such a solution, construction of a population model is essential.

Spatial characteristics of mechanoreceptive fibers are being investigated widely [12, 13, 14, 15, 16], because the knowledge about the spatial response properties of individual mechanoreceptive fibers is important to construct accurate and adequate population models for these afferents. However, recent population model studies used uniform response profiles (symmetric response characteristic in all axes) for afferents and space-invariant attenuation functions which were dependent only on the distance between the contactor location and the receptive field center.

In their population model study, Güçlü and Bolanowski (2005) concluded that the actual attenuation function also should be dependent on the specific location of the receptive field center, because the mechanics of the skin vary along the phalanx [1].

Thus, response profiles of mechanoreceptive afferents may change related to the mechanical properties of the skin. Findings of Goodwin et al. (1995) and Ray and Doetsch (1990) showed asymmetric response profiles in proximo-distal and cauda-lateral axes.

In addition, the innervation density increases towards the fingertip [17, 18, 19]. Therefore lower psychophysical thresholds would be expected distally, but the psychophysical detection thresholds do not improve towards fingertip [1]. Thus, there may be a (mechanical or physiological) factor that may counterbalance the effects of innervation density which is higher distally.

Finally, recent population models run on vibratory stimulations, but there are only a few studies which used mechanical vibratory stimulations to inspect the response profiles of mechanoreceptive fibers. Therefore, a well understanding of response profiles of mechanoreceptive fibers under vibratory stimulation is necessary.

1.2 Objectives

The objective of the thesis presented here is to test the mechanoreceptive fiber response profile under vibratory stimulus and test the hypotheses that responses of mechanoreceptive fibers are not symmetric along the proximo-distal axis.

1.3 Outline

The thesis is presented as follows: In chapter 2, background information about the sense of touch, the structures and functions of skin and mechanoreceptors, and the skin mechanics are given. In chapter 3, experimental procedures are explained. In chapter 4, results are presented. In chapter 5, discussion of results is interpreted.

2. THEORY

Senses -sight, hearing, touch etc.- are the physiological capabilities of organisms that provide inputs for perception. There is a specific sensory system dedicated to each sense. Receptors, together with their central pathways and target areas in the brain, comprise a sensory system, and the activity within a system gives rise to a specific type of sensation such as touch, taste, vision, or hearing. Sensory systems are responsible for processing specific sensory information such as amount of light, chemicals or skin deformation. Because of the continuous changes that occur around an individual, each sensory system is assigned to provide an up-to-date representation of the external world.

While the senses differ in their modes of reception, all the senses share two common steps [20]:

- A physical stimulus, and
- A set of events transforming the stimulus into nerve impulses.

Ascending mechanisms begin with the activity of peripheral receptors, which together form an initial neural representation of the external world. Descending mechanisms work to sort out those events that require immediate attention from the large amount of sensory input [21].

2.1 Sense of Touch

The term of touch is used to define the physical contact between two objects. In everyday experience, one perceives the sense of touch when an object applies physical force upon his/her body, or vice versa. Since the human skin is lined with mechanical receptors, skin is the main organ that is responsible for the sense of touch.

In our everyday lives, there are a number of functions which we regularly perform with touch. We use the information that rises from the sense of touch to grasp and manipulate tools and other objects with considerable dexterity. Without this sensory input, we drop things and frequently hurt ourselves. In the absences of some senses, we use touch. For example, touch is used to identify objects, and to learn about the spatial layout of objects and surfaces near the body. In addition, a deaf person can use touch to sense the vibration on the diaphragm of a speaker to feel the music. We also use touch to assess various perceptual attributes of objects, particularly surface texture, hardness, thermal qualities, weight, and movement of an object's parts. It is also possible to determine shape, size, and function of objects.

2.2 Physiology

The sense of touch is provided by afferent neurons innervating the skin in different layers (Figure 2.1), so both skin and mechanoreceptors have roles in the sense of touch.

2.2.1 The Skin

Skin is the largest organ in the body with a weight of 5 kg and surface area of 2 m^2 in a 70-kg individual [22]. Human skin consists of a stratified, cellular epidermis and an underlying dermis of connective tissue. Subcutaneous fat lies beneath the dermis, and it is separated from the rest of the body by muscle tissue.

The epidermis is mainly composed of keratinocytes, and its thickness is typically 0.05-0.1 mm. Indeed, 80-90% of the mass of the epidermis is comprised by keratin and filaggrin. The dermis has a thickness that varies from less than 0.5 mm to more than 5 mm. Collagen, as the main extracellular matrix protein, comprises 80-85% of the dry weight of the dermis. Skin is an elastic material which can be stretched reversibly by 10-50%. [22]

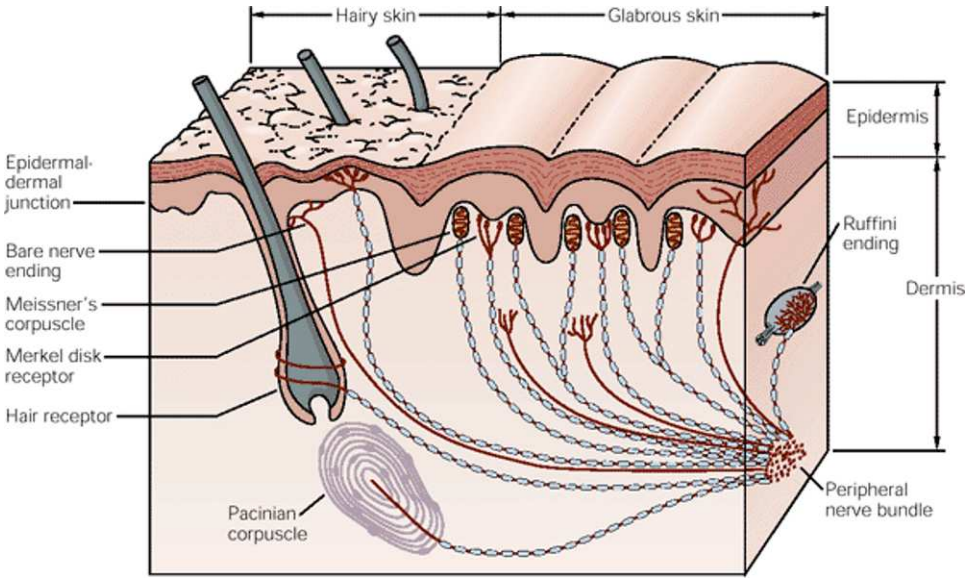

Figure 2.1 An illustration of mammalian hairy and glabrous skin in Principles of Neural Science, 4th edition [23].

The skin is innervated by a dense, three-dimensional network of highly specialized afferent and efferent nerve branches. Functionally specific afferent units were discovered in electrophysiologic studies [24]. Two major categories of afferent units have been clearly established: mechanoreceptors and thermoreceptors [25, 26]. A third group of pain receptors (nociceptors) respond only to high-threshold stimulation, including mechanical, thermal (heat pain) or chemical stimulation. There are also polymodal nerves that respond to more than one modality. Within each of these categories some of functionally different afferent units can be clearly identified with their morphologically distinct structures [22]. The sensory nerves innervating the skin serve the sensations of touch, vibration, pressure, change in temperature (warmth and cold), pain (including heat pain) and itch [27, 28].

2.2.2 Mechanoreceptors

Each form of energy must be transduced by a population of specialized cells, which convert the stimulus into a signal that all neurons understand. In each sensory system the initial contact with the external world occurs through specialized neural structures called sensory receptors . The sensory receptor is the first cell in each sensory

pathway, and it transforms stimulus energy into electrical energy. The electrical signal produced by the receptor is termed the receptor (generator) potential [20] or spike. The amplitude and duration of the receptor potential are related to the intensity and time course of stimulation of the particular receptor. The process by which specific stimulus energy is converted into an electrical signal is called stimulus transduction [20].

Receptors are morphologically specialized to transduce specific forms of energy. Each receptor has a specialized anatomical region where stimulus transduction occurs. Most sensory receptors are optimally selective for a single stimulus energy, a property termed receptor specificity. The unique stimulus that activates a specific receptor at a low energy level was called an adequate stimulus by Charles Sherrington [20].

The sensory system that is responsible for the sense of touch is the somatosensory system. It consists of mechanoreceptors, afferent pathways, and somatosensory cortex. Receptors which transduce mechanical stimulation -such as pressure and vibration- into receptor potential are called mechanoreceptors.

Touch is mediated by mechanoreceptors in the skin, there being two main functional groups [26, 29] according to the way they respond to sustained constant stimulus. Slowly adapting mechanoreceptors respond continuously to a persistent stimulus, whereas rapidly adapting (fast adapting in human) mechanoreceptors respond at the onset and frequently at the end of the same stimulus, but not throughout the sustained part of the stimulus [30]. Thus, the slowly adapting mechanoreceptors respond to static skin indentations with a sustained discharge, whereas the rapidly adapting mechanoreceptors respond only during the dynamic phase of the skin deformation.

Glabrous and hairy skins have different types of mechanoreceptor. The hair-follicle receptors are predominant mechanoreceptors in hairy skin. The glabrous skin (e.g. the hairless skin of the palmar surface of the hands) is innervated by two main types of superficial mechanoreceptor: the Meissner corpuscles as rapidly adapting receptors, and the Merkel cells as slowly adapting receptors [29, 30]. Subcutaneous tissue and the deeper dermis of both hairy and glabrous skin contain two types of mechanoreceptors: the Pacinian corpuscle, which is a rapidly adapting receptor; and Ruffini ending, which is a slowly adapting receptor [29]. In contrast to the small receptive-field (RF) size of Meissner corpuscles and Merkel cells in the upper dermis, the RFs of

Pacinian corpuscles and Ruffini endings are large [29]. Also innervation densities of PCs and Ruffini endings are less than those of Meissner corpuscles and Merkel cells [29]. Thus, while the Meissner corpuscles and Merkel cells signal a more detailed image of the skin deformation due to their smaller RF size and higher innervation density, Pacinian corpuscles and Ruffini endings signal a more global image due to their larger RF size and lower innervation density.

- **Meissner Corpuscles and Rapidly Adapting Type I Afferents**

Figure 2.2 A photography of Meissner corpuscle with nerves supplying it within the dermal papilla of a 24-year-old man (maginification: x220) by Rindley [31].

Meissner corpuscles (Figure 2.2) are the end organs of rapidly adapting afferents (RA, denoted as FAI in human), and they encapsulate the unmyelinated nerve endings of these afferents. Each corpuscle consists of a number of flattened layers of supportive cells arranged as horizontal lamellae which are then surrounded by a connective tissue capsule. Nerve endings form a coil-like structure among the Meissner corpuscles. When the corpuscle is deformed by pressure, the nerve endings are stimulated registering the sensation of touch. Meissner corpuscles are located within the dermal papillae which are the finger-like projections of the dermis into the epidermis (Figure 2.1). Dermal projections into the epidermis places the RAs as close to the surface of the skin as is possible within the dermis. This proximity, particularly, accounts for the high

sensitivity of RAs to instantaneous skin deformation. Johansson and Vallbo (1979) showed that the innervation density of RAs is 141 afferents/cm^2 in the finger tip, and decreases to 25 afferents/cm^2 in the palm [17]. In the study of Darian-Smith and Kenins (1980) on monkey index finger, they found the innervation density as 178 afferents/cm^2 in the distal phalanx while this value decreases to 80 afferents/cm^2 in the middle phalanx [19].

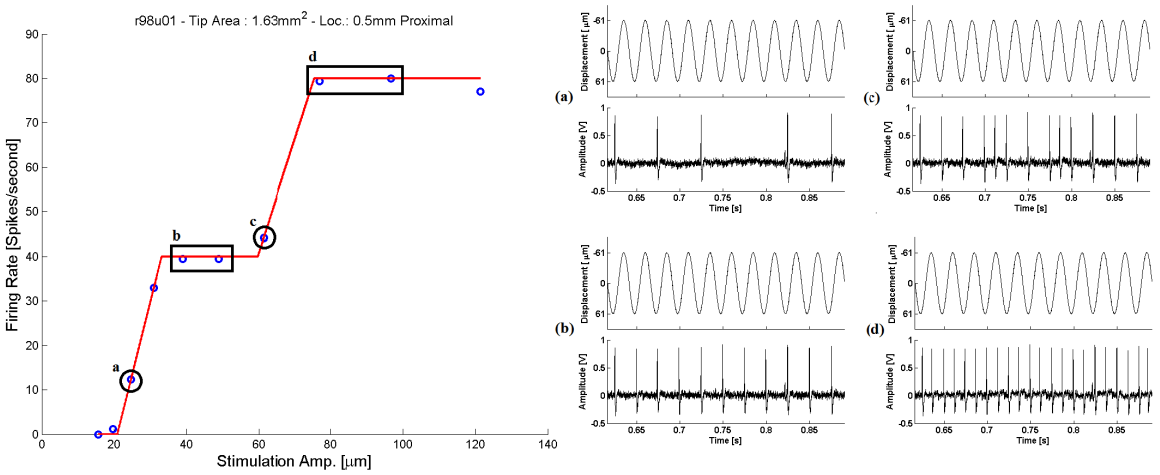

Figure 2.3 Rate-intensity function and discharge pattern of an RA (r98u01)

RAs are very sensitive to even the slightest stretch of the skin, as happens when an object slips in the hand. RAs are poorer than SAIs at resolving the spatial details of objects, but, on the other hand, they are better at resolving vibrotactile patterns. RAs' sensitivity is high at a frequency near 40 Hz [32, 33, 34]. There is a consistent correlation between this type of response and the structure of the afferent axon and its surrounding tissue. The connective tissue acts as a mechanical filter that eliminates the components of persistent stimulus on the nerve ending. Thus, RAs are more likely to inform the timing of the stimulus. They fire a few spike at the onset and offset of a sustained stimulus, and they may entrain with a vibratory stimulus and fire one or two spikes per cycle. Entrainment is the action of generating one or more spikes per stimulation cycle. In Figure 2.3, rate-intensity function and discharge patterns of an RA (r98u01) is shown. At the first entrainment level, mechanoreceptive fiber generates one AP at positive half of each stimulation cycle (Figure 2.3.b). At the second entrainment level, mechanoreceptive fiber generates one AP at each half of stimulation

cycle (Figure 2.3.d).

Rapidly adapting response characteristic of these afferents make them inappropriate for form and texture perception; instead, they may be responsible for the detection of objects slipping across the hand and fingers [35], thus they may provide the sensory information that leads to the adjustment of grip force [36, 35].

• Merkel Cells and Slowly Adapting Type I Afferents

Merkel cells are the end organs of slowly adapting type I afferents (SAI). Each SAI axon branches onto the tip of several closely packed epidermal ridges in glabrous skin (Figure 2.1). Each branch has a series of axon terminals. Axon terminals run towards the Merkel cells where an expanded nerve plate is associated with each tactile cell (Figure 2.4). Merkel cell and axon terminal form the Merkel cell-neurite complex (MCN) which contains a chemical synapse. Also, Merkel cells contain vesicles filled with glutamate and serotonin being released when the receptor is mechanically stimulated [37]. Clusters of Merkel cells result in a surface elevation which is called a touch dome in the skin of cats and in the hairy skin of humans [36].

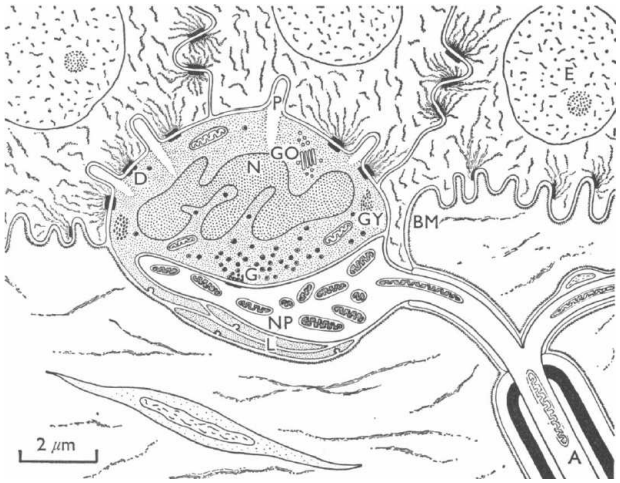

Figure 2.4 A diagram of Merkel cell-neurite complex depicted by Iggo and Muir [38]. A, myelinated axon; BM, basement membrane; D, desmosome; E, epithelial cell nucleus; G, granular vesicles in the tactile cell near a junction with the nerve plate, NP; GO, Golgi apparatus; GY, glycogen; L, lamellae underlying the nerve plate; N, multilobulated nucleus; P, cytoplasmic process from the Merkel Cell.

SAIs are characterized with small RFs, and irregular, long lasting discharge pattern under a persistent stimulus [38, 32, 39]. The response of an SAI is highly localized; the area of skin from which this response could be evoked is small and discrete.

SAIs also feature the response property of surround suppression [15]; stimulation of the surrounding tissue together with RF center results a mechanical inhibition of SAI response, so RFs of SAIs show minimal growth with increasing stimulus amplitudes [14]. SAIs have low mechanical thresholds, and their firing rates are dependent on the velocity and amplitude of the displacement. There is a period of rapid adaptation before a sustained response which may continue for >30 min when a persistent stimulus is presented [38]. SAIs are more sensitive to static indentations and low frequency vibrations (<8 Hz) [32], and also their sensitivity at lower frequencies than 4 Hz is better than Meissner corpuscles [40]. Thus, SAIs contribute to the detection of frequencies below 4 Hz.

The MCN together with Merkel cell-skin interaction gives rise to the SAI selectivity to a particular component of local stress-strain field, which makes it sensitive to edges, corners, and curvature of objects. Surround suppression property of individual SAIs results, psychophysically, in greater sensitivity to surface features -such as curvature- than to uniform and flat surface indentations [15]. Since SAI responses are independent of the force, psychophysical pattern recognition is also independent of contact force [35]. In addition to the fact that their innervation density is high (70-134 afferents/cm^2 at the fingertip in man and monkey [17, 19, 35]), spatial resolution of an individual SAI is capable of resolving spatial detail of 0.5 mm, although their receptive field diameters are 2-3 mm [35]. Thus, SAIs may be responsible for processing the form and texture information of objects [36, 35].

- **Ruffini Endings and Slowly Adapting Type II Afferents**

Ruffini endings are spindle-shaped mechanoreceptors within which axons of afferent fibers terminate (Figure 2.5). These mechanoreceptors give rise to the second type of slowly adapting response; SA type II (SAII). Direct recordings were done from the peripheral nerves of humans in some studies, but they do not exist in monkeys or mice [36, 35]. Johansson and Vallbo (1979) found the innervation density of SAII afferents in the human hand approximately 50 afferents/cm^2 [17].

An SAII differs from an SAI in the greater size of its RF, reduced sensitivity to simple indentation of the skin, the greater sensitivity to the skin stretch, and regular

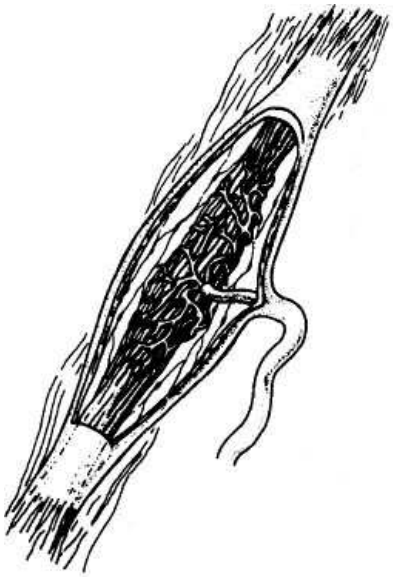

Figure 2.5 Diagram illustrating the structure of Ruffini ending. Outer capsule has a window cut to expose fluid-filled subcapsular space and core of nerve fiber terminals, Schwann cells, and collagen fibrils [41]

firing pattern under persistent stimulus [32]. When compared with SAIs, SAIIs have approximately five times larger RFs, and also they are approximately six times less sensitive to skin indentation, but 2-4 times more sensitive to skin stretch [35].

SAIIs take role in the perception of the direction of the motion or force when any skin stretch occurs. When an object is moved over the skin surface, it produces local skin deformations. While the SAIs signal the local deformations, SAIIs signal a neural image of the skin stretch which may define the direction of the movement. Deepness of the receptor prevents the domination of skin indentations over skin stretches which is used to perceive the direction of object motion. Another function of SAIIs takes place in the perception of the hand shape and the finger position together with muscle spindles and joint afferents [35]. The pattern of the skin stretch as a result of any hand and finger position is signaled by SAIIs.

- **Pacinian Corpuscles and Pacinian afferents**

Unmyelinated tip of each Pacinian afferent (PC in rat, monkey and cat; FAII in human) ends in a Pacinian corpuscle. The Pacinian corpuscle is distinct with its onion-like structure (Figure 2.6). It serves as a connective tissue that filters low frequency mechanical stimulus, such as sustained pressure applied to the skin. The lamellae

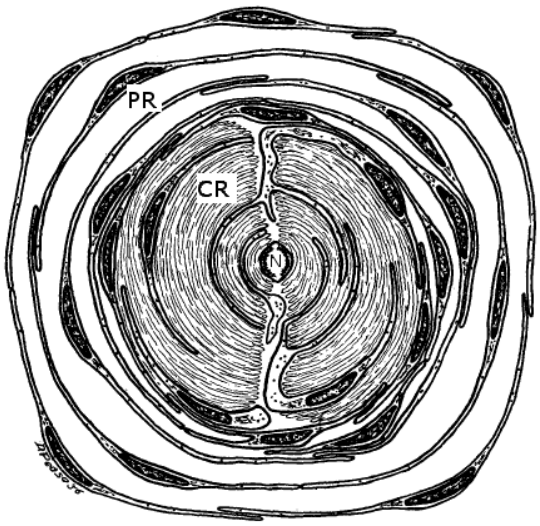

Figure 2.6 Diagram illustrating the cross-section structure of Pacinian corpuscle. The bare nerve ending (N) is surrounded by lamellae which is seperated into two regions: Core region, CR; and Peripheral region, PR [43]

that form the corpuscle are actually modified versions of Schwann cells. In the fluid-filled center of Pacinian corpuscle is unmyelinated nerve ending. If the outer core of connective tissue that surrounds the bare nerve ending is dissected, the axon itself is capable of generating a steady burst of action potentials with continued application of a probe [36]. A change in structure of the fluid-filled capsule may carry the energy of a persistently applied probe away from the axon tip in miliseconds. But Pawson et al. (2009) find the clues for glial-neuronal interaction which is mechanochemical rather than purely mechanical [42]. In contrast to static indentation, when a repeated mechanical stimulus is applied, such as vibration, a series of discrete transduction events and a series of action potentials (AP) occur.

PCs basically differ from RAs by their large RF sizes, which may cover an entire organ -such as glabrous skin of rat hind paw of a rat [32]. In addition, they discharge less APs than that RAs do at the onset and offset of static indentations. Also their preferred frequency is higher than that of RAs. But there is one property that is common for both mechanoreceptors: entrainment.

Although PCs operate at higher frequencies, they may synchronize with vibratory stimulus of frequency between 100-150 Hz [35]. Leem et al. (1993) also reported PCs responding to each cycle of a 300-Hz sinusoidal stimulus of 20-μm amplitude superimposed on a 300-μm steady indentation of the skin [32].

When PCs are tested with uniform or constant-velocity displacement, one or two impulses result only at the onset of stimulus, but sinusoidal displacement (vibration) generates a regular stream of impulses [30]. They display a high responsiveness between 200-300 Hz [32, 35]. Thus, PCs are responsible to signal high frequency vibration even at smallest magnitude, and this feature turns them into a detector of remote events. These are the receptors, for example, that respond as hands gripping a steering wheel vibrate when a car travels over a rough road [36]. The most sensitive PCs respond to vibratory amplitudes as small as 3 nm applied directly to the corpuscle and 10 nm applied to the skin [35]. However, PCs' spatial resolution is too low because of the deep location in the dermis [35]. Also, their innervation density was found by Johansson and Vallbo (1979) as 20 afferents/cm^2 in the finger tip, 10 afferents/cm^2 in the remaining of the finger, and 10 afferents/cm^2 in the palm [17].

The most important function of PCs for human is to signal distant events transmitted through objects, probes, and hand-held tools [44]. When we become skilled in the use of a tool, we perceive events at the working surface of the tool via these afferents as though our fingers were present [35].

- **Types of Touch Afferent Fibers**

All somatosensory information from the limbs and trunk is conveyed by dorsal root ganglion neurons and the information rises from cranial structures (the face, lips, oral cavity, conjunctiva, and dura mater) is transmitted by the trigeminal sensory neurons, which are functionally and morphologically homologous to dorsal root ganglion neurons.The cell body of neuron lies in a ganglion on the dorsal root of a spinal nerve. The axon has two branches, one projecting to the periphery and one projecting to the central nervous system. The terminal of the peripheral branch of the axon is the only portion of the dorsal root ganglion cell that is sensitive to natural stimuli and the remainder of the peripheral branch, together with the central branch, is called the primary afferent fiber [23]. Mechanoreceptors and proprioceptors are innervated by dorsal root ganglion neurons with large-diameter, myelinated axons that conduct action potentials quickly. Thermal receptors and nociceptors have small-diameter axons that are either unmyelinated or thinly myelinated and these nerves conduct impulses

more slowly [23]. These differences in fiber size are important physiologically, because they affect the speed at which action potentials are conducted to the brain.

All tactile fibers, which are mechanoreceptors defined in previous sections, conduct action potentials in the Aβ (type II) range which covers the velocities between 35-70 ms^{-1} [44]. Axons of these mechanoreceptive fibers are myelinated and have a diameter between 6 and 12 μm [45].

The clinician takes advantage of the known distribution of conduction velocities of afferent fibers in peripheral nerves to diagnose diseases that result in degeneration of the fibers. In certain conditions there is a selective loss of axons; in diabetes, for example, large sensory fibers degenerate (large-fiber neuropathy). This selective loss is reflected in a reduction in the peak of the compound action potential, a slowing of nerve conduction, and a corresponding diminution of sensory capacity. Similarly, in multiple sclerosis the myelin sheath of large-diameter fibers degenerates, producing slowing of nerve conduction or failure of impulse transmission. [23]

2.2.3 Coding of Stimulus by Somatosensory System

As all sensory systems, somatosensory system conveys four basic types of information when stimulated; modality, location, intensity, and timing. Together, these four elementary attributes of a mechanical stimulus produce the sensation of touch. These attributes of sensory experience are encoded within the nervous system by specialized subgroups of neurons.

- **Modality**

The modality defines a general class of stimulus which is determined by the type of energy transmitted by the stimulus and the receptors specialized to sense that energy [20, 21]. The specificity of response in receptors underlies the labeled line code; the most important coding mechanism for stimulus modality [20, 21]. Receptor's selectivity for a particular type of stimulus energy means that the axon of the receptor functions as a modality-specific line of communication; activity in the axon necessarily

conveys information about a particular type of stimulus. Excitation of a particular sensory neuron, whether naturally or artificially by direct electrical stimulation, elicits the same sensation [20, 21]. In a particular population of somatosensory neurons' activity -for example the activity of cutaneous mechanoreceptors- is always interpreted by the central nervous system (CNS) as touch, no matter whether the stimulus is natural (an object placed on the skin) or artificial (stimulation of the appropriate axons with electrical current).

The somatosensory system consists of five distinct modalities: touch, proprioception -limb position sense and muscle tension information, temperature sense, pain [46]. Each of these major modalities has several constituent qualities or submodalities. Submodalities exist because each class of receptors -chemoreceptors, mechanoreceptors, and thermoreceptors- is not homogenous. Instead, each class contains a variety of specialized receptors that respond to a limited range of stimulus energies . Texture, pressure and vibration may be considered as some of submodalities of touch [46]. Texture of a surface is supposed to be signaled by the superficial mechanoreceptors: SAIs and RAs. Pressure is assumed to be signaled mainly by SAIIs, but SAIs may also take part in this action. Vibration may be signaled as three different frequency bands by mechanoreceptors of PCs, RAs, and SAIs. As mentioned in previous section (Section 2.2.2), PCs might be responsible to signal high frequency vibrations while RAs might be responsible for sensing low frequencies and SAIs might be responsible for sensing very low frequencies.

- **Location**

The individual receptors are incapable of signaling the stimulus location [16], instead, the location of the stimulus is represented by the population of sensory receptors within the sensory system. Receptors are distributed topographically in a sense organ so that their activity signals not only the modality of the stimulus but also its position in space and its size. In the skin, the density of cutaneous receptors varies markedly across the skin surface. The greatest density of afferent endings was found at the fingertips and the mouth, whereas receptors along the surface of the back were less frequent [21].

Spatial awareness involves three distinct perceptual abilities [20]:

- Locating the site of stimulation on the body,
- Discriminating the size and shape of objects, and
- Resolving the fine detail of the stimulus or environment.

These spatial abilities are linked to the structure of the RF of each sensory neuron. The position of the RF is an important factor in the perception of the location of a stimulus on the body. The RF of a sensory neuron in somatic sensation assigns a specific topographic location to the sensory information. The RF of a cutaneous mechanoreceptor is the region of the skin directly innervated by the terminals of mechanoreceptive afferents and its size can change based on stimulus properties. Thus it includes the entire area of the skin through which a tactile stimulus can be conducted to reach the nerve terminals. [20]

Each receptor responds only to stimulation within its RF. A stimulus that affects an area larger than the RF of one receptor will activate adjacent receptors. Therefore, the size of a stimulus affects the total number of receptors that are stimulated. For example, a large object, such as a basketball, held between both hands will contact and activate more touch receptors than a pencil grasped between the thumb and index finger.

Resolution of the sensory system in a given body part is determined by the density of receptors in that area. Receptors in a dense population of the same receptors have smaller RFs, which leads to finer resolution of spatial detail. The spatial resolution of a sensory system is not uniform throughout the body, because the receptor density changes from one body part to another. For example, spatial discrimination is very acute in the finger tips, where sensory receptors are plentiful and the RFs are small. In other regions, such as the trunk, the spatial information signaled by individual nerves is less precise because receptors in those areas are fewer and thus have larger RFs. [23]

- **Intensity**

For a given afferent, the intensity of the stimulus is signaled by its firing rate -frequency of action potentials generated at receptor terminal. The firing rate of an afferent reflects the total amount of stimulus energy delivered to the receptor. The perceived intensity arises from an interaction between the number of neurons activated by a stimulus and the firing rate of these active neurons. Therefore, the number of activated neurons together with the activity level of these neurons gives rise to an intensity code.

The intensity or amount of a sensation depends on the strength of the stimulus. The capacity of sensory systems to extract information about the magnitude of the stimulus is important for two aspects of sensory discrimination [20]:

- Distinguishing among stimuli that differ only in strength (as opposed to those that differ in modality or location) and
- Evaluating the stimulus amplitude.

- **Timing**

The timing of stimulation is defined by when the response in the receptor starts and stops, and it is determined by how quickly the energy is received or lost by this receptor [20].

- **Receptive Field in Touch**

The receptive field is the specific region of a sensory organ (eye, skin, tongue etc.) that can elicit neuronal responses when stimulated. In touch, receptive field of a mechanoreceptive fiber defines a certain restricted region of the skin mechanical stimulation of which makes fiber respond. Likewise, in vision, receptive field of an optic fiber defines a certain restricted region of the retina illumination of which makes fiber respond. However receptive field of optic fibers consit of two distinct regions;

center and surround. For on-center fibers illumination of center region excites the fiber while illumination of surround region inhibits the response of the fiber. For off-center fibers reverse is true. On the other hand, mechanoreceptive afferents do not have such distinct excitatory and inhibitory regions, although it is valid for cortical neurons. Vega-Bermudez and Johnson (1999) studied the receptive field structure of SAI and RA afferents and showed that RF structures of these afferents were not uniform and region stimulution of which elicite afferent response grows as the amplitude of the stimulation increases and multiple hot-spots (maximal response points) occur [14]. Thus determining the RF maps according to the maximal response is not confidential. In stead, finding the region of skin which makes the fiber respond with a minimum stimulation amplitude is more confidential.

2.3 Skin Mechanics

When one touches an object, the perceived tactile information results from the population response of mechanoreceptive fibers responding to the spatio-temporal distribution of mechanical loads on the skin. These loads and the resulting stresses and strains at where mechanoreceptors within the skin are have roles in the neural coding of tactile information, because the mechanoreceptors that are embedded in the skin and the belonging subcutaneous tissue respond to the local compressive and shear strains [15, 47].

Mechanical properties of the skin is determind by its composition. The extracellular matrix (ECM) is the largest component of normal skin and gives the skin its unique properties of elasticity, tensile strength and compressibility [48]. The ECM is composed of a variety of polysaccharides, water and collagen proteins. On a weight basis, the tensile (breaking) strength of normal skin approaches that of steel, yet skin also has substantial elasticity and compressibility [48]. These properties are due to the combination of fibrous structural proteins and proteoglycans.

The skin is an anisotropic, viscoelastic, nonlinear, highly deformable and low compressible material [47, 49, 50, 51, 52, 53, 54, 55]. Its strain-stress curve is not linear under tensile loading (Figure 2.7), but it can be expressed as two phases [49, 50, 51,

53, 54];

- For small strains, low stiffness
- For large strains, high stiffness

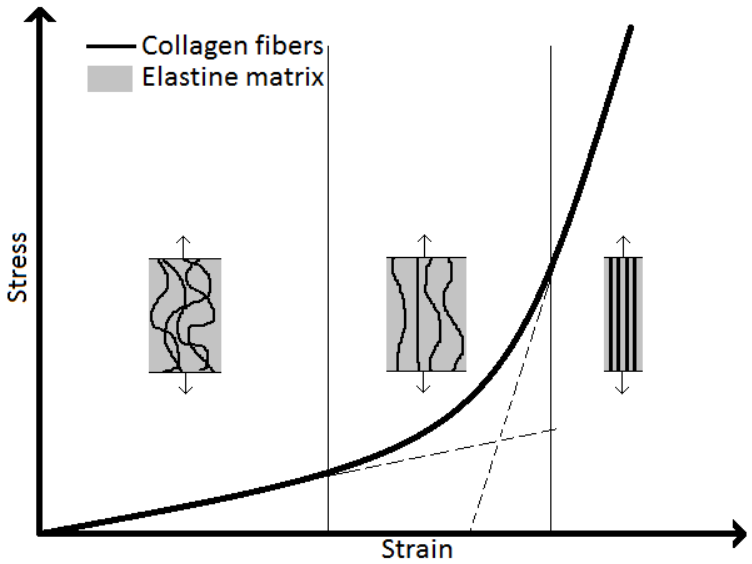

Figure 2.7 Graph and subdiagrams illustrating the behavior of collagen fibrils, elastine matrix and stress-strain curve under tensile loading. Redrawn referencing figure by Dellaleau et al. [50]

Collagen fibers in the ECM of the skin are crimped at rest, therefore, elastin fibers dominate the linear behavior of the skin at low strains. Elastin fibers presents highly linearity which gives the property of high deformability of the skin. During this linear region (phase one), elastin fibers determine the strength of the skin, and collagen fibers get oriented in almost parallel with the direction of stretching [49, 50, 54]. Phase two can be divided into two distinct parts; one is nonlinear "toe" region and other is nearly linear region [53]. Once the collagen fibers are sufficiently aligned, further extension of the skin requires stretching of these collagen fibers. Extension of collagen fibers cause a significant increase in stiffness [22, 54]. Strength of the skin at "toe" region is determined by the cumulative effects of straightened collagen fibers and elastin fibers. Once all collagen fibers are straightened, both collagen and elastin fibers are stressed, then the high elastic modulus of collagen fibers modifies the elastic response of the skin, which becomes stiffer [50].

Elastin fibers are less rigid and more extensible than collagen fibers; they can

be reversibly stretched to more than 100% [53]. Therefore, elastin fibers support the recovery of the skin shape by acting as highly efficient "springs" which store mechanical energy.

Studies on the skin and tendon suggest that proteoglycans contribute primarily to the mechanic response at low and intermediate levels [53]. Also they play a role during the displacement of the interstitial fluid and interacts with collagen fibers, therefore it is an element of the viscosity of the skin [50]. Although, in daily physiological loading conditions, the skin of hands and fingers are predominantly in compression, however skin's compressibility is small [51, 55]. Incompressibility of the skin can be attributed to the proteoglycans.

From a more global perspective, the skin undergoes large deformations while the daily handling of objects and exploratory touching. For example, fingerpad of a human can experience significant amount of deformation [47];

- Fingertip tapping at 0.5 Hz results in 0.75 N of normal force and 1.5 mm of normal deformation.
- A shearing force of 1.9 N can induce approximately 4 mm of tangential deformation.
- Fingertip sliding on a flat glass surface experiences a local tangential deformation of 30%.

However, the experiments here use small strains; 0.1 N of compressive strain results from a vibratory stimulation with a frequency of 40 Hz and a peak amplitude of 62 μm superimposed on a 0.5 mm preindentation.

Skin has good frictional properties, assisting locomotion and manipulation by its texture [56]. Güçlü and Bolanowski (2005) showed that the mechanical impedance of the skin is not constant along proximo-distal axis [1]. This nonuniform distribution of mechanical impedance can be attributed to the anisotropic property of the skin. Nonuniform mechanical impedance distribution implies the change of stiffness and resistance of the skin through the body. Therefore, the attenuation function of the skin

cannot be constant but changing as a factor of location [1], and each mechanoreceptor in the skin would be exposed to a different amplitude of stimulation according to its location relative to the stimulation point.

In mechanics, skin can be represented as a spring (k), a damper (b) and a mass (m). These components determines the stiffness, the resistance and the inertia of the skin. Example of a basic mechanical model (Kelvin-Voigt) of skin is seen in Figure 2.8. There are also other models used to estimate mechanical behavior of the skin consisting of the components mentioned above. When the force is applied, behavior of k is related to the displacement whereas behavior of b is related to velocity, and m is related to acceleration. The force on this particular mechanical model is expressed as in Eq.2.1

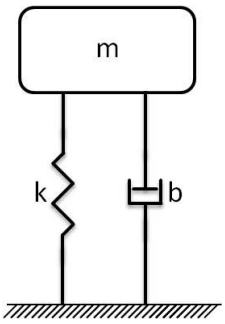

Figure 2.8 A basic mechanical model used to represent the skin's mechanical properties. The skin has a mass (m), spring (k) and damper (b) components.

$$F = m\ddot{x} + b\dot{x} + kx \tag{2.1}$$

These mechanical components (the mass (m), the stiffness (k) and the resistance (b)) are results the skin's mechanical impedance (Z). Regardless of the model used, Z can be expressed in terms of the force (F) and the velocity (v) applied to the skin together with the phase difference between them (ϕ) (Eq.2.2).

$$Z = \frac{F}{v} \times e^{-i\phi} \tag{2.2}$$

where

$$F = F_0 e^{iwt}, \quad v = v_0 e^{i(wt+\phi)} \tag{2.3}$$

Eq. 2.2 enables us to express Z in terms of resistance and reactance as in Eq. 2.4.

$$Z = Re\{Z\} + jIm\{Z\} \tag{2.4}$$

where $Re\{Z\}$ is the resistance, and $Im\{Z\}$ is the reactance of the skin. Resistance is defined as resulting from energy dissipation within the system. Reactance is defined as resulting from storage of either kinetic or elastic energy, which is released in another phase of the time-varying cycle. [57]

3. METHODOLOGY

Rats have been studied frequently in electrophysiologic studies of mechanoreceptors in mammalian skin [32, 39, 53]. Rat was chosen in this study too due to its convenience in handling and experiments compared to other mammalians.

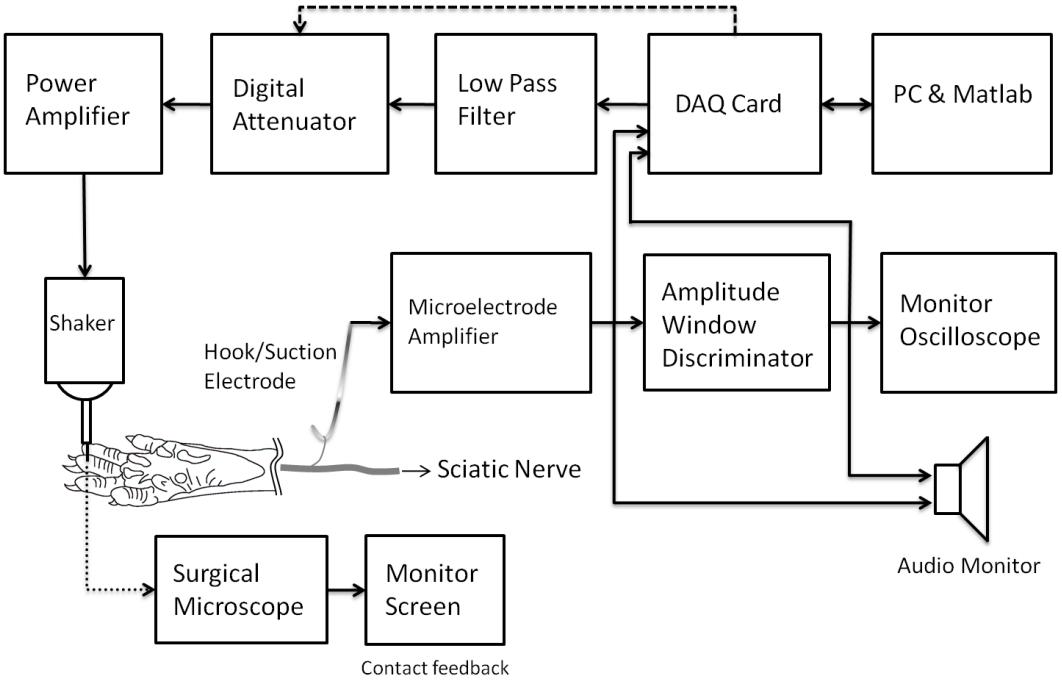

(a)

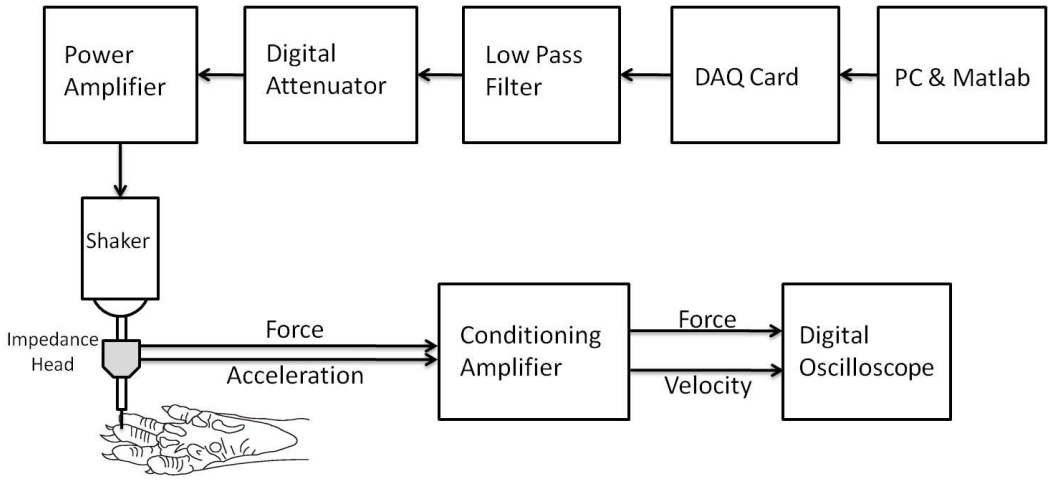

(b)

Figure 3.1 Block diagrams of electrophysiological experiment (a) and mechanical impedance measurement (b) setups.

3.1 Animals

30 adult Wistar rats of either sex (15 males and 15 females), about 178-393 g in weight were used in this study. They were held in cages with 12-h light/dark cycles and fed with pellet feed. The experiments were approved by Bogazici University Institutional Ethics Committee for the Local Use of Animals in Experiments.

Of these 30 rats, one male rat weighting 205 g was used for mechanical impedance measurements, and remaining 29 rats were used solely in electrophysiological experiments.

3.2 Equipment

The block diagram of the electrophysiological experiment setup is shown in Figure 3.1(a). A custom-made MATLAB (The MathWorks, R2008a) code was used to generate the stimulus pattern, to record the raw data and the timing of APs generated by mechanoreceptive fibers. The amplitude of the stimulus was controlled by the software. The digital acquisition card (DAQ) (National Instruments) was used to convert the digital stimulus pattern coming from MATLAB into analog signal and analog signals coming from recording device into digital signals. The low pass filter (LPF) was used to filter high frequency noise in the stimulus signal. The cut-off frequency of the LPF was set to 1 KHz. The digital attenuator (ISR Active Attenuator) was used to adjust the amplitude of the stimulus. Its attenuation level (in dB) was set by MATLAB code or manually. A custom-made power amplifier was used to drive the shaker (Ling Dynamic System, model: V101). The shaker was mounted on a custom-made structure and a boom stand. It could be positioned in all three axes and lowered onto the skin. Plastic contactors were used to stimulate the skin. A platinum hook electrode or a suction electrode which contained an Ag-AgCl electrode was used for recording APs from nerve strands. A custom-made microelectrode amplifier with the gain options of 1000 and 10000 was used to amplify APs. The amplitude window discriminator (WPI-121) was used to discriminate the APs of a single afferent if necessary and convert them

into pulses. The monitor oscilloscope (Hitachi) was used to monitor nerve activity together with discriminator window levels. The sound monitor was used to hear the nerve activity. A Faraday cage (1.58x1.05x1.20 m) provided an electromagnetic shield, and a floating table provided mechanical insulation of the setup from environment. Von Frey hairs were used to map the RF centers of mechanoreceptive afferents and also to classify them.

The block diagram of mechanical impedance measurement setup is shown in Figure 3.1(b). A Type 8001 (Brüel and Kjær,) impedance head was used to measure the mechanical impedance of the skin. A Nexus Type 2692 conditioning amplifier (Brüel and Kjær) was used to filter, amplify and calibrate the acceleration and the force signals from the impedance head. The velocity and the force signals from conditioning amplifier were measured on the digital oscilloscope (Tektronix) screen.

3.3 Electrophysiological Procedure

3.3.1 Surgery

Rats were anesthetized with an induction dose of 60-75 mg/kg ketamine and 10 mg/kg xylazine intraperitoneally (IP). Supplementary doses (1/3 of induction dose) were given as required. Upper hind limbs of rats were depilated with hair removal cream before surgery. After the rats were placed on the surgical table, their rectal temperature, respiration rate, and pedal and eye-blinking (palpebral) reflexes were monitored. Body temperature was kept at 37°C by a thermostatically controlled heating pad (Physitemp).

Once the rat's condition was stabilized (respiration rate was regular and rectal temperature was $\sim$ 37°C), the hind paw which would be studied was fixed with modelling clay. The glabrous skin of the hind paw was facing up. Upper leg dorsal skin and muscle was incised 3 mm cauda-lateral of ischium, and the sciatic nerve was exposed. A pool was made with retractors, and it was periodically flushed with Krebs-Henseleit solution (112 mM NaCl, 4.6 mM KCl, 1.9 mM $CaCl_2$, 1.1 mM $MgSO_4$, 0.8 mM KH_2PO_4, 24 mM $NaHCO_3$, and 10 mM D-glucose adjusted to pH 7.2-7.4). The

sciatic nerve was cut from proximal end. Perineurium was dissected, and the nerve bundle was placed on the hook electrode to check the tactile activity while touching the glabrous skin.

If the nerve was dry and the activity was lost, the leg was sutured and the other leg was operated on. After recording from both legs the animal was euthanized with 200 mg/kg thiopental IP. Death was confirmed by lack of the heart beat and respiration.

3.3.2 Single Unit Search and Classification

Sciatic nerve was dissected until a single unit responding to glabrous skin touch was isolated. Once this was achieved, its RF center was found with the smallest von Frey hair to which the unit responded. RF center of the unit was marked on a diagram.

The mechanoreceptive fibers were classified according to their adaptation rates under static indentation applied with a supra-threshold von Frey hair, and according to their RF sizes. Classification criteria for each type of mechanoreceptive afferent were as the following:

- Fibers which discharged at the onset and offset but not at the sustained portion of stimulus, and had spot-like RFs were classified as RAs.
- Fibers which discharged at the onset and offset but not at the sustained portion of stimulus, and had big RFs were classified as PCs.
- Fibers which had sustained discharge under static stimulus were classified as SAs.

No further sub-classification of SAs was done, because it was difficult to do classification on pads based on the RF size. In addition, during the quick classification protocol, there was no controlled ramp-and-hold stimulus to sub-classify SAs according to their inter-spike-interval (ISI) histograms.

3.3.3 Mechanical Stimulation

Sinusoidal mechanical vibrations (Figure 3.2) superimposed on a 0.5-mm static indentation were applied perpendicular to the hind paw glabrous skin. 0.5-mm preindentaion was used to prevent decoupling of contactor and skin. Rise and fall times of the vibration burst were 50 ms, and the duration between half-power points was 0.5 s. Sinusoidal vibration bursts increased and decreased as $\cos^2$ functions. There was a 0.5-s interval before the mechanical stimulus. The total duration of one trial was 2 s (Figure 3.2(a)). Inter-stimulus-interval was 3 s.

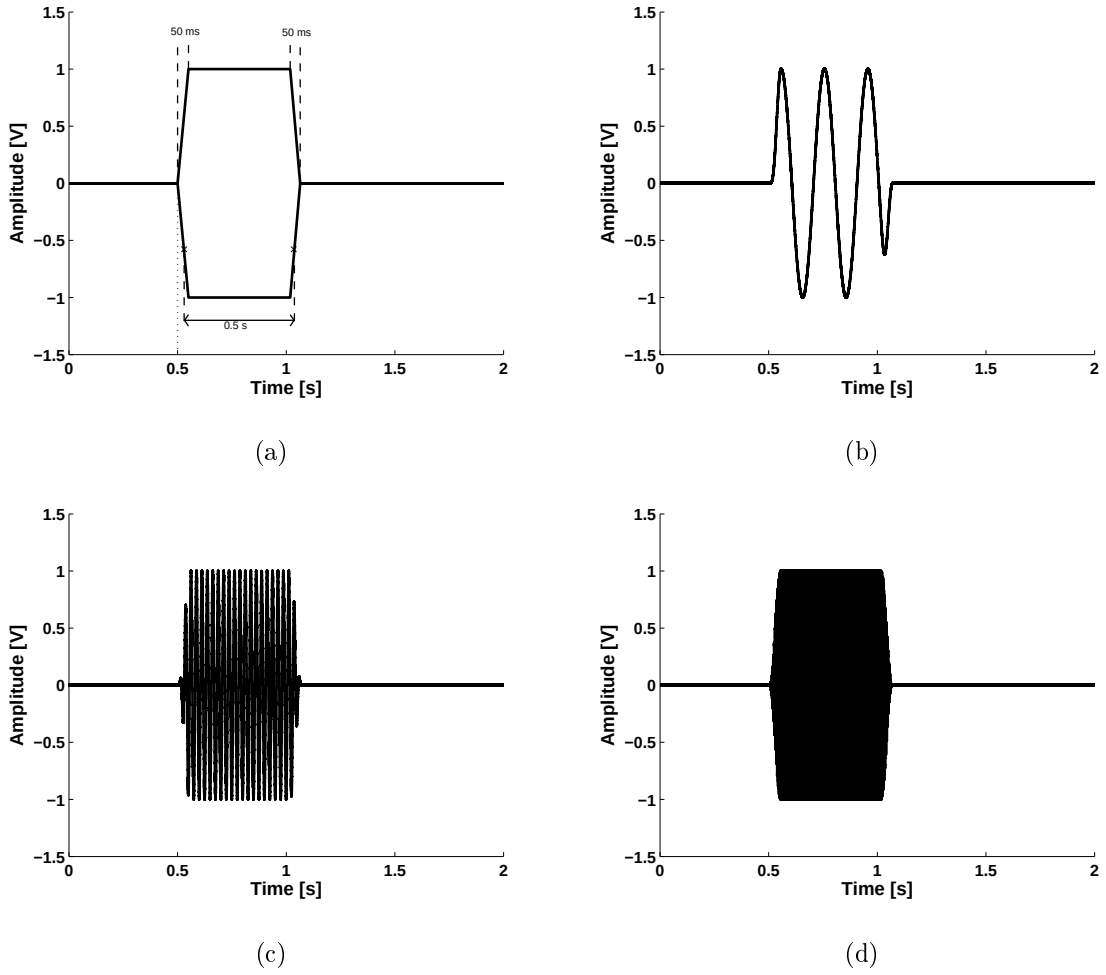

Figure 3.2 Mechanical Stimulus; (a) Rise and fall times were 50 ms, and the duration between half-power points was 0.5 s. Sinusoidal vibration bursts increased and decreased as $\cos^2$ functions. There was a 0.5-s interval before the mechanical stimulus. The total duration of one trial was 2 s. (b) A 5-Hz mechanical vibration was applied for SAs; (c) a 40-Hz mechanical vibration was applied for RAs; (d) a 250-Hz mechanical vibration was applied for PCs.

Frequency of the stimulus was chosen according to the type of mechanoreceptive afferent. The frequency was set to:

- 5 Hz, if an SA was being studied (Figure 3.2(b)).
- 40 Hz, if an RA was being studied (Figure 3.2(c)).
- 250 Hz, if a PC was being studied (Figure 3.2(d)).

However, this thesis primarily involves data from RA fibers. RF maps and sample counts of SAs and PCs were given for information.

Five different stimulus locations relative to the RF center (2 distal, 1 RF center, 2 proximal) (Figure 3.3) and three different contactor sizes (area: 0.39 mm^2, 1.63 mm^2, 2.96 mm^2) were used. Each condition (location and contactor size combination) was tested with 10 amplitude levels at 4 repetitions. To avoid decoupling of the skin and contactor, amplitudes greater than 250 μm were rarely used [58]. In this thesis, the spatial properties of mechanoreceptive fibers were study only in proximo-distal axis. To study spatial properties in cauda-later axis was not appropriate due to larger contactor size relative to smaller finger width. Also, due to time restrictions, additional mesurements in cauda-lateral axis was not realistic.

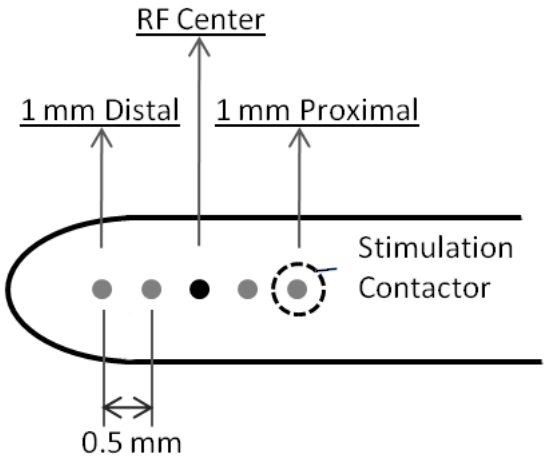

Figure 3.3 Finger illustration showing the stimulation of rat glabrous skin at 5 different locations relative to RF center of mechanoreceptive afferent in proximo-distal axis.

3.3.4 Recording

Contactors were randomly chosen in order to eliminate the effects of persistent adaptation of skin structure due to the sustained deformation. Stimulator was lowered on the RF center and indented 0.5 mm beyond the initial contact point. Although there are studies in which contactors were sticked to skin surface, we prefer to pre-indent the skin not to change the nature of behavior of the skin under vibratory stimulus. MATLAB code ran and attenuation level was set manually from attenuator to observe adequate spikes. Levels of amplitude window was adjusted from discriminator, so that peaks of APs of a single unit were within window. APs and amplitude window levels were observed on the oscilloscope to ensure that all APs were captured. Amplitude window levels were adjusted as necessary during the experiment. The audio monitor was also used to hear activity of unit during recording. The absolute spike threshold level was determined by manually changing the attenuation level. Initial attenuation level of MATLAB code was set to an attenuation level to which unit did not respond. Final attenuation level and decrement steps were chosen so that 10 attenuation levels were tested. 4 repetitions were set for each attenuation level. The frequency was set according to the type of afferent (see Section 3.3.3). Stimulation and recording were automated by MATLAB code. This procedure was repeated for each location and contactor. The skin was let to relax between trials. A MATLAB file containing stimulation parameters and spike timings was saved after each recording.

3.3.5 Data Analysis

Average firing rates of RAs for each attenuation level was calculated based on 4 repetitions. Rate-intensity functions were constructed for each unit at each possible stimulation location with three different contactor sizes. Rate-intensity data sets were fitted by piecewise linear functions by regression (Figure 3.7). The parameters of absolute spike threshold (a_0) and entrainment threshold (a_1) were obtained from fitted rate-intensity functions. These parameters were plotted as a function of stimulus location and contactor area.

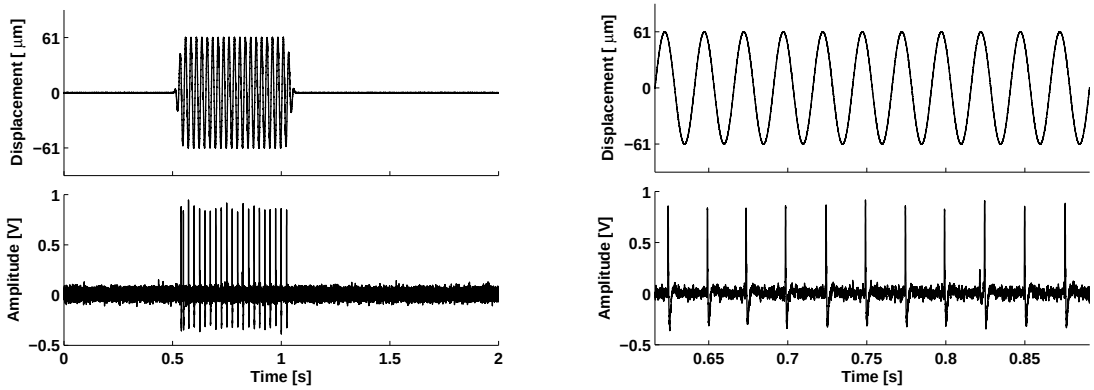

(a) (b)

Figure 3.4 (a) Graphs showing the APs generated by an RA (r67u01) stimulated with 40-Hz mechanical vibration at RF center. (b) Mechanoreceptive afferent was entrained with mechanical vibration in 1-for-1 pattern.

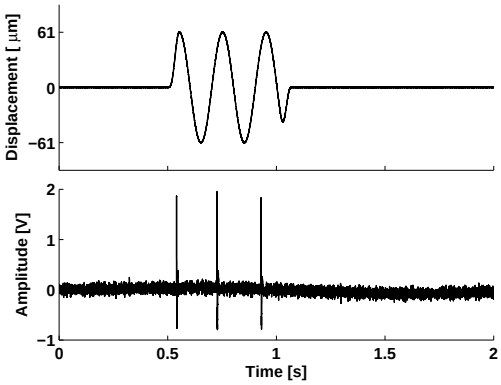

Figure 3.5 Graph showing the APs generated by an SA (r48u01) stimulated with 5-Hz mechanical vibration at RF center.

No analysis were performed for SAs and the PC, because the sample sizes were too small.

3.4 Mechanical Impedance Measurement Procedure

3.4.1 Animal Preparation

The rat on which mechanical measurements were done was anesthetized with an induction dose of 60 mg/kg ketamine and 10 mg/kg xylazine intraperitoneally (IP).

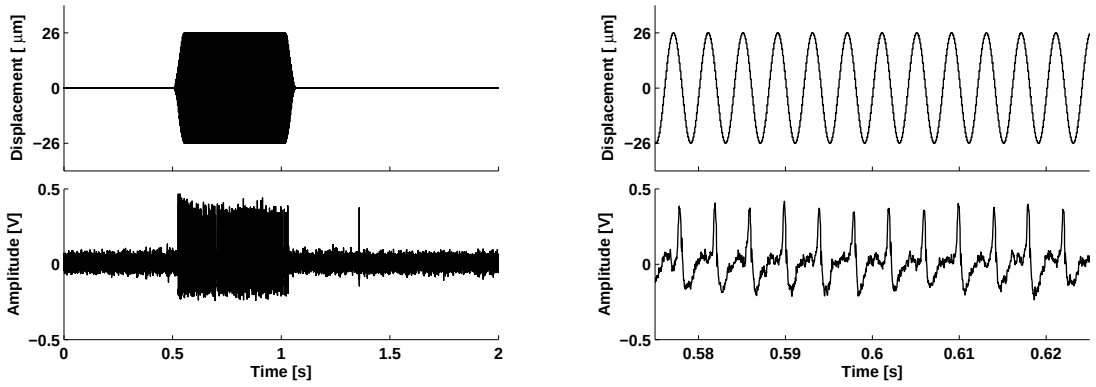

(a) (b)

Figure 3.6 (a) Graphs showing the APs generated by a PC (r60u03) stimulated with 250-Hz mechanical vibration at RF center. (b) Mechanoreceptive afferent was entrained with mechanical vibration in 1-for-1 pattern.

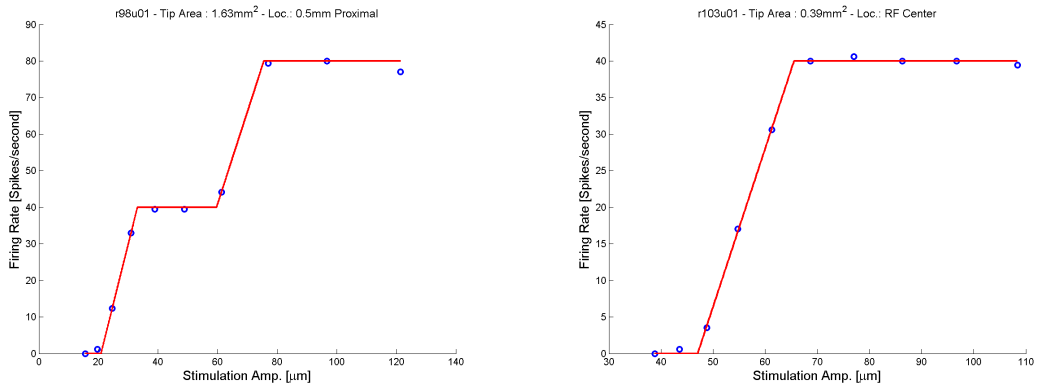

(a) (b)

Figure 3.7 Graph showing the rate-intensity functions of two RAs stimulated with 40-Hz mechanical vibration; (a) r98u01, (b) r103u02.

Supplementary doses (1/3 of induction dose) were given as required. After the rat was placed on the experiment table, its rectal temperature, respiration rate, and pedal reflexes were monitored. Body temperature was kept at 37°C by the heating pad. The left hind paw was fixed with modelling clay; glabrous skin was facing up. No surgical operations were done; after the measurements were completed, rat was allowed to recover.

3.4.2 Mechanical Stimulation and Impedance Measurement

A 40-Hz vibrotactile stimulation (Figure 3.2(c)) with an amplitude of 61μm (the mean absolute spike threshold of RAs at RF center with smaller contactor, see Chapter 4) was used for mechanical impedance measurements. The glabrous skin of left middle finger of rat's hind paw was stimulated at five different locations in proximo-distal axis (distance from fingertip: 0.5 mm, 1 mm, 1.5mm, 2 mm, and 2.5 mm) with a small contactor (area: 0.41 mm^2) (Figure 3.8). The velocity (v) and the force (F) values from conditioning amplifier were recorded for each location at 5 repetitions.

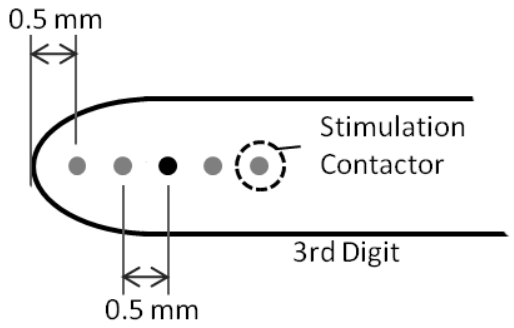

Figure 3.8 Finger illustration showing the locations of mechanical impedance measurements; Skin's mechanical impedance was measured at 5 different locations relative to the fingertip in proximo-distal axis.

The complex ratio of F to v gives the mechanical impedance (Eq.2.2). The model shown in Figure 2.8 was used to estimate mechanical components of the skin. The resistance and reactance components were estimated with Eq.3.1 and Eq.3.2.

$$b = Re\{Z\} \tag{3.1}$$

$$(m_s w - k/w) = Im\{Z\} - m_{con} w \tag{3.2}$$

where m$_s$ is the mass of the skin and m$_{con}$ is the mass of the contactor used to stimulate the skin.

The impedance, the resistance and the reactance were plotted as a function of location to see the impedance profile of the skin in proximo-distal axis.

3.5 Statistical Analysis

2-way ANOVA was used to test any significant effects of stimulation distance and contactor size on RA response parameters (a_0, a_1). Post-hoc Tukey test was used to test significant differences between parameters at different locations regardless of contactor size, and parameters with different contactors regardless of contactor location.

No statistical analysis were applied to SA and PC samples, because the sample sizes were too small.

4. RESULTS

4.1 Distribution of Mechanoreceptive Afferents in the Rat Hind Paw Glabrous Skin

A total of 77 mechanoreceptive afferents was classified from 29 rats' hind paw glabrous skin, and their RF centers were mapped on rat hind paw figure (Figure 4.1(a)). Percentages of mechanorecetive afferent types among classified sample were shown in Table 4.1(a). The most frequent observed afferent type was RA (85.7%), and its observation rate increased distally. This observation was congruent with the findings of morphological studies [17, 18, 19]. Only one PC was observed, which was expected because PCs innervation density through the skin is very low [17] relative to those of other mechanoreceptors.

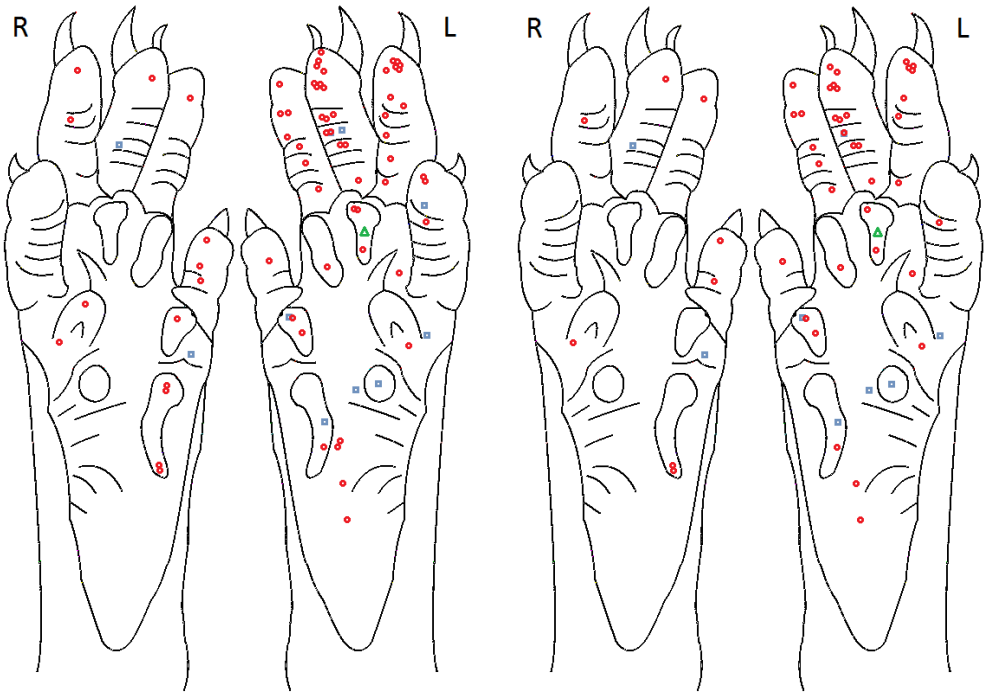

(a) (b)

Figure 4.1 Receptive field maps of; (a) 77 classified mechanoreceptive afferents, and (b) 54 recorded mechanoreceptive afferents on the rat hind paw glabrous skin. Red circles show RA-Is, blue rectangles show SAs, and the green triangle shows the PC.

Of 77 classified afferents, 54 afferents' response were recorded under mechanical stimulation (Figure 4.1(b)). Percentages of mechanorecetive afferent types among recorded sample were shown in Table 4.1(b).

Table 4.1
Percentages of tactile afferent types among; (a) the classified sample, and (b) the recorded sample.

(a)

Afferent Type	Digit	Palm	Pad	Total	Percentage %
RA	46	7	13	66	85.7
SA	4	3	3	10	13
PC	0	0	1	1	1.3
	50	10	17	77	100

(b)

Afferent Type	Digit	Palm	Pad	Total	Percentage %
RA	32	5	8	45	83.3
SA	2	3	3	8	14.8
PC	0	0	1	1	1.9
	34	8	12	54	100

No significant effects related to gender and weight were found. Also there was no significant difference between parameters of mechanoreceptive fibers recorded from left and right paw.

4.2 Effect of Location and Contactor Size

Number of afferents of which response was recorded with each possible location and contactor size combination was shown in Table 4.2 for each afferent type. Sample numbers were not balanced due to the lost of afferent activity or the location of the RF center which was either too close to edges or on a pad.

Table 4.2
Sample numbers at each location and contactor size for each afferent type.

Contactor area [mm^2]	0.39					1.63					2.96				
Stimulation distance [mm]	1P	0.5P	0	0.5D	1D	1P	0.5P	0	0.5D	1D	1P	0.5P	0	0.5D	1D
RA	24	29	43	18	17	17	18	30	16	14	17	17	28	14	13
SA	1	3	8	3	2	2	2	5	2	1	2	2	5	2	2
PC	0	0	1	0	0	0	0	1	0	0	0	0	1	0	0

4.2.1 Response Profile of RA Fibers in Proximo-Distal Axis

Figure 4.2 shows the absolute spike threshold and entrainment threshold profiles along proximo-distal axis with different contactor sizes. Both absolute spike threshold and entrainment (one action potential for one stimulation cycle) threshold of whole RA sample showed an asymmetric change as the stimulation distance from RF center increased in both directions for all contactor sizes, but this asymmetry was less obvious for entrainment threshold with the contactor size of 2.96 mm^2. The same trend was valid for thresholds of RA sample innervating only the digit glabrous skin.

For whole RA sample, 2-way ANOVA showed that the effect of stimulus location on absolute spike thresholds was statistically significant ($p<0.001$) and there was no interaction between the contactor size and the stimulus location ($p=0.792$). Differences between absolute spike threshold for 1-mm proximal and those for RF center, 0.5-mm and 1-mm distal were significant ($p<0.05$) based on post-hoc Tukey test (Figure 4.3(a)). Also absolute spike thresholds for 0.5-mm proximal and 0.5-mm distal were significantly different ($p<0.05$). There were no significant differences among the remaining pairs of stimulus locations for absolute spike thresholds. The effect of stimulus location on the entrainment threshold was significant ($p=0.034$, 2-way ANOVA) and there was no interaction between the contactor size and the stimulus location ($p=0.119$). Post-hoc Tukey test showed that the only significant difference in the entrainment threshold was between 1-mm proximal and 0.5-mm distal stimulus locations ($p<0.05$) (Figure 4.3(b)).

For RA sample innervating the digit glabrous skin, 2-way ANOVA showed that the effect of stimulus location on absolute spike thresholds was statistically significant ($p<0.001$) and there was no interaction between the contactor size and the stimulus

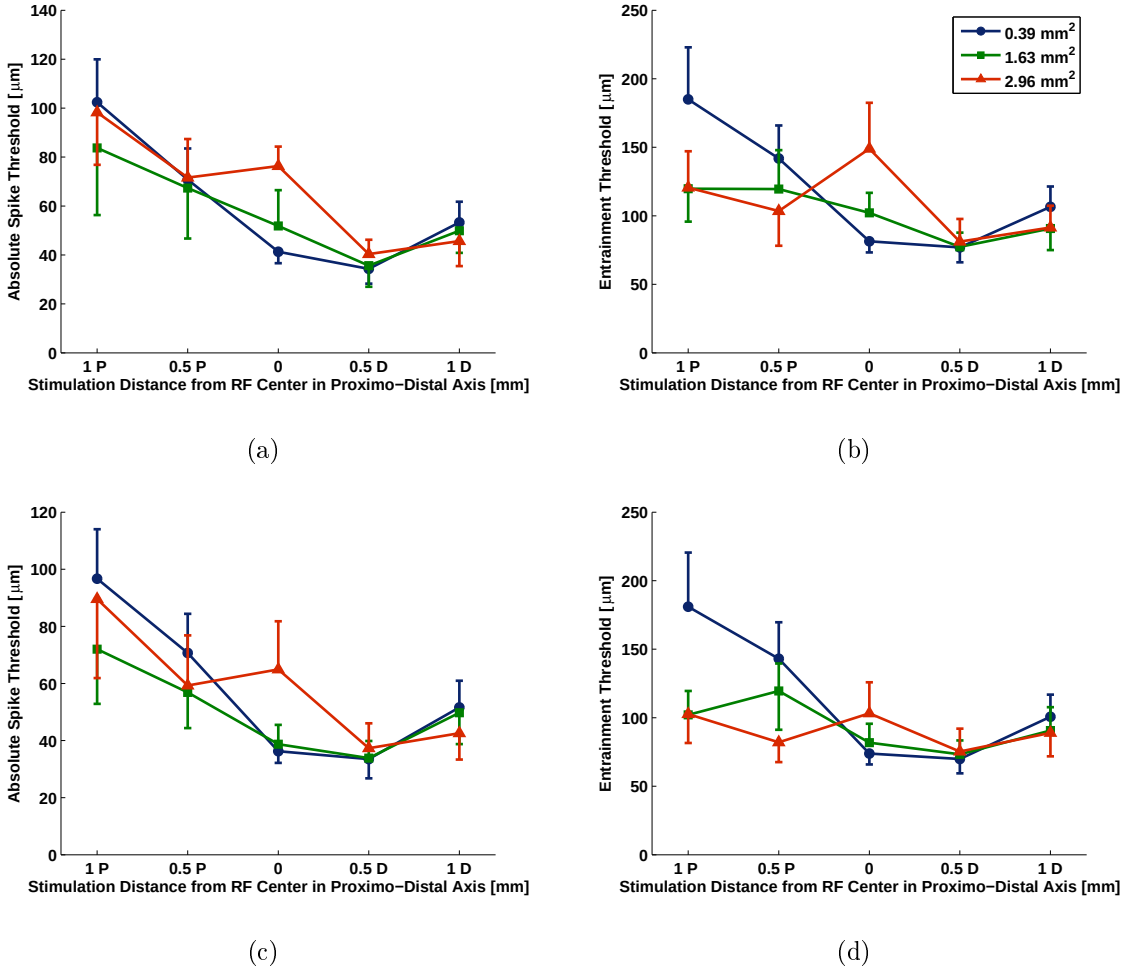

Figure 4.2 Graphs showing the effect of stimulation distance from RF center; (a) and (b) show the absolute spike threshold and entrainment threshold profiles of whole RA sample, respectively. (c) and (d) show the absolute spike threshold and entrainment threshold profiles of the RA sample innervating only the digit glabrous skin, respectively.

location (p=0.814). Differences between absolute spike thresholds for 1-mm proximal and those for RF center, 0.5-mm and 1-mm distal were significant ($p<0.05$) based on post-hoc Tukey test (Figure 4.3(c)). There were no significant differences among the remaining pairs of stimulus locations for absolute spike thresholds. The effect of stimulus location on the entrainment threshold was significant (p=0.022, 2-way ANOVA) and there was no interaction between contactor size and stimulus location (p=0.187). Post-hoc Tukey test showed that the only significant difference in the entrainment threshold was between 1-mm proximal and 0.5-mm distal stimulus locations ($p<0.05$) (Figure 4.3(d)).

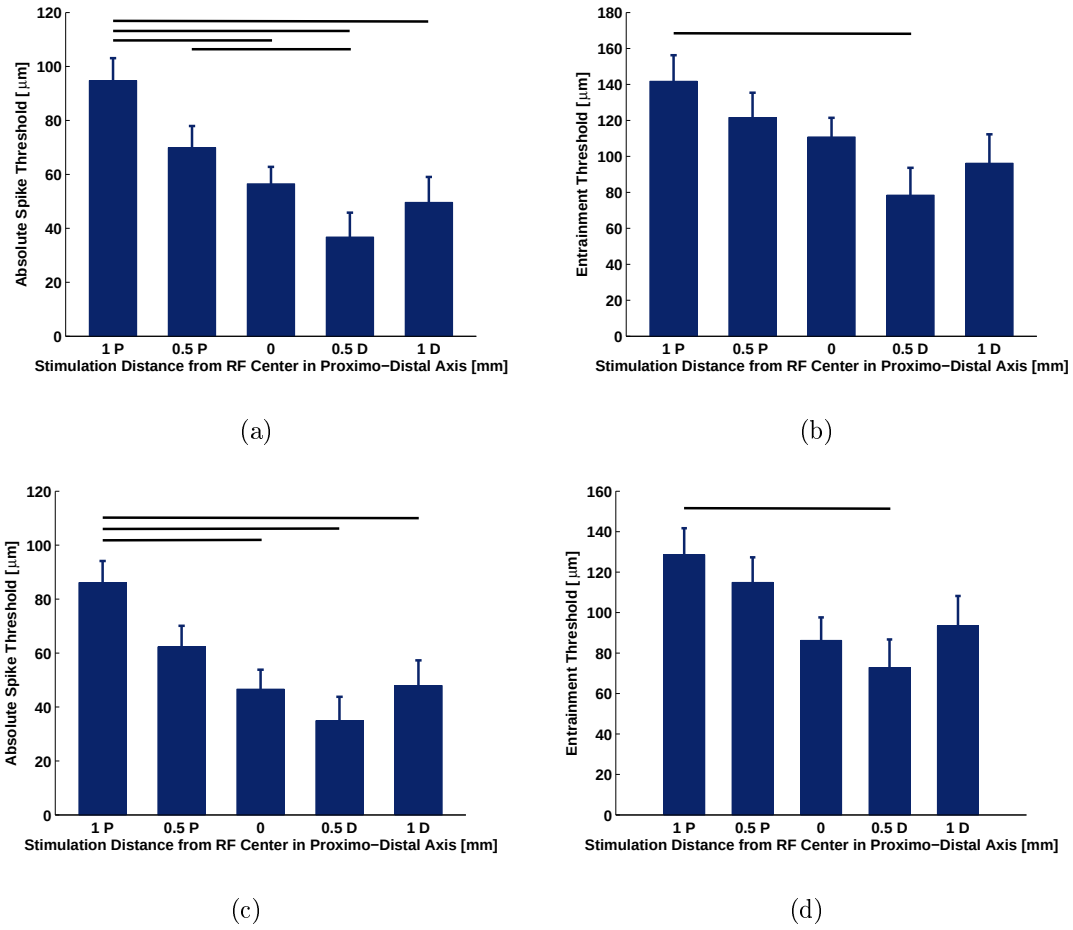

Figure 4.3 Graphs showing Tukey Test results for location factor; (a) and (b) show the significant differences for whole RA sample absolute spike threshold and entrainment threshold profiles, respectively. (c) and (d) show the significant differences for absolute spike threshold and entrainment threshold of RA sample innervating the digit glabrous skin, respectively. Lines above the bars shows the significant differences ($p<0.05$).

4.2.2 Response of RA Fibers Under Different Contactor Sizes

Figure 4.4 shows the effect of contactor size on absolute spike threshold and entrainment threshold for whole RA sample and RA sample innervating the digit glabrous skin. In all cases, increment of contactor area resulted in increment of thresholds for RF center. At distant locations entrainment threshold decreased as the contactor area increased, whereas absolute spike threshold decreased at 1-mm distal stimulation, but showed a u-shaped behavior at 1-mm proximal stimulation.

2-way ANOVA showed that the effect of contactor size on absolute spike thresholds and entrainment thresholds for both whole RA sample and RA sample innervating the digit galbrous skin was not significant (whole RA sample; $p=0.642$ for a_0, $p=0.54$

for a_1, RA sample innervating the digits; p=0.603 for a_0, p=0.186 for a_1).

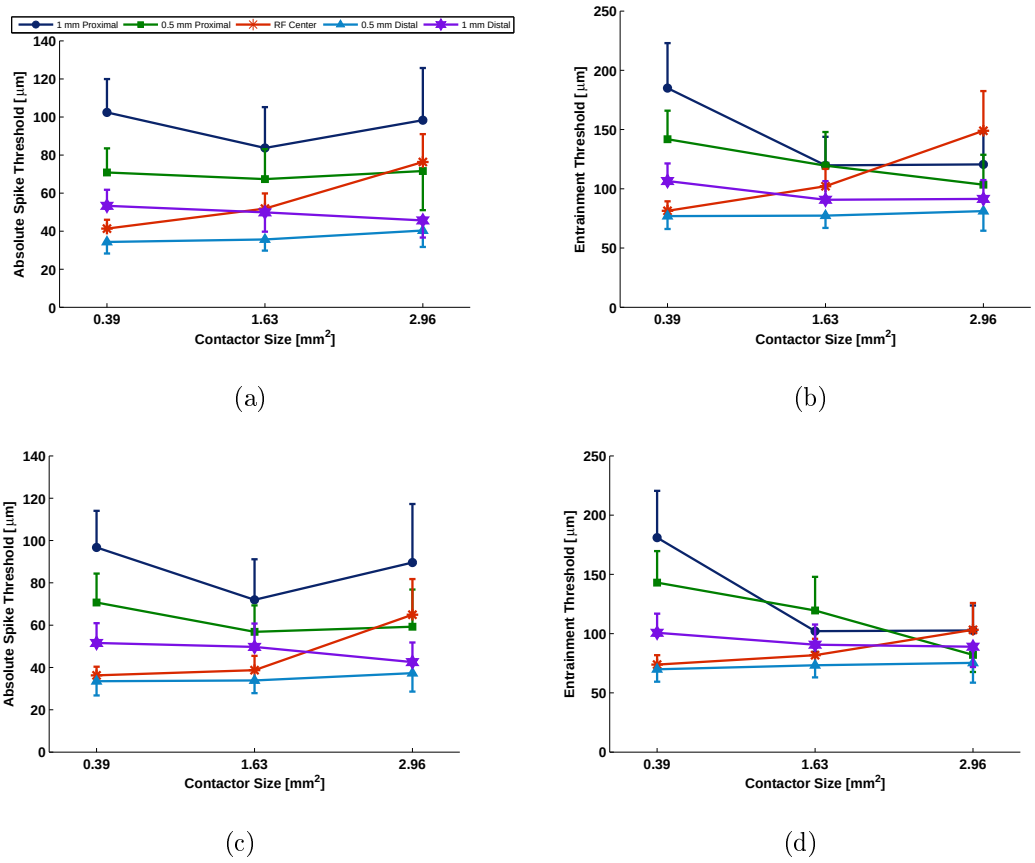

Figure 4.4 Effect of contactor size on RA (a,c) absolute spike threshold and (b,d) entrainment threshold. (a,b) Response profile for whole RA data. (c,d) Response profile for RAs innervating the glabrous skin of rat foot digits.

4.3 Mechanical Impedance of the Rat Glabrous Skin

4.3.1 Impedance Profile of Skin Along Proximo-Distal Axis

The impedance profile of distal phalanx of rat's hind paw at 40 Hz is shown in Figure 4.5 as averages of five measurements at each point (±SE). The impedance of the skin was not uniform along proximo-distal axis, instead it increased proximally.

The resistance was found to govern the impedance of skin. It had a maximum value at the most proximal of phalanx where the skin lies on the muscle and bone and gets thinner. This means that highest energy dissipation occurs at proximal end of the phalanx. The reactance of the skin due to its mass and stiffness was much smaller

than the resistance. In distal locations skin thickness is greater than that in proximal locations, because the skin gets thinner as it lies on bone and muscles. Furthermore, in histological pilot experiments on rat glabrous skin slices, Gok et al. (2011) showed that boundaries between epidermal layers were not clear and cells were in a more stiff arrangement in proximal slices when compared to distal slices [59]. A more stiff arrangement of cells might result in a reduction in stiffness (spring-like property) of the skin by reducing stiffness constant. Thus reactance might be due to the stiffness in distal locations, whereas it might be due to the domination of the mass of skin as the stiffness approaches to zero in proximal of the phalanx (Figure 4.5).

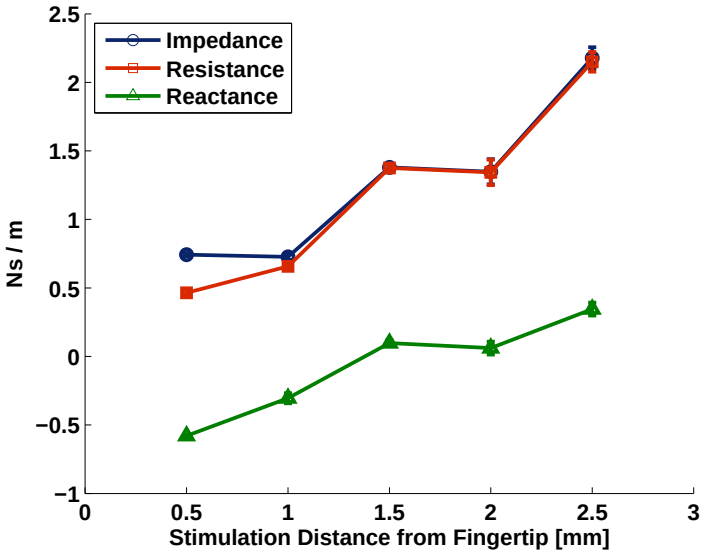

Figure 4.5 Graph showing the change of impedance ($|Z|$), resistance ($Re\{Z\}$), and reactance ($Im\{Z\}$) as a function of the location at 40 Hz.

4.3.2 Mechanical Model

Although the contactor size was small enough to measure point impedance of the skin, mechanical impedance measurements involved additional horizontal components, such as stiffness due to the stretch of surface of the skin. These additional components have role in the spread of mechanical stimulus through the skin. This condition was modeled as in Figure A.1. Mathematical and computational background is given in Appendix A and B.

Mechanical system that was modelled had more unknowns than the equations,

so simplifications and known parameters were needed. Physiological data were used to estimate in what ratio stimulus spreads in proximal and distal directions. In order to use this data, it is assumed that a mechanoreceptor was activated if a displacement equal to the mechanorecetor's threshold achieved at the RF center, no matter where the stimulator is located. Electrophysiologic measurements of this study showed that a mean of 41.323-μm displacement was enough to activate an RA stimulated at the center of its RF, and also a mean of 102.399-μm and 53.285-μm displacements were enough to activate an RA stimulated at 1-mm proximal and 1-mm distal locations, respectively. According to the assumption, at each stimulation location, the resultant displacement at the RF center was equal to the threshold of the RA stimulated at its RF center (41.323 μm). For instance, when a stimulus of 102.399 μm is applied at 1-mm proximal relative to the RF center, stimulus will spread towards RF Center (in distal direction), and a resultant displacement of 41.323 μm will occur at RF center. In the same manner, a stimulus of 53.285 μm at 1-mm distal relative to the RF center will produce a displacement of 41.323 μm at the RF center. If we assume that the attenuation in one direction is uniform (direction selectivity), the attenuation coefficient in distal (or proximal) direction will be equal to the ratio of threshold of the RA stimulated at its RF center and threshold of the RA stimulated at 1-mm proximal (or distal) location (Eq. 4.1).

$$Attenuation\,Coefficient = \frac{Mean\ a_0\ at\,RF\,Center}{Mean\ a_0\ at\,1-mm\,Distant} \tag{4.1}$$

Also, the reactance ($Im\{Z\}$) of the skin was assumed to be uniform through the skin, because the impedance of the skin was governed by the resistance and reactance did not vary too much compared to the resistance (Figure 4.5).

As a result with the assumption that $Im\{Z_0\}$=$Im\{Z_1\}$=$Im\{Z_2\}$, k_{21} was found to be greater than k_{01}, and the resistance of the skin was found to be increase proximally ($Re\{Z_0\} < Re\{Z_1\} < Re\{Z_2\}$) (Table 4.3).

Table 4.3
Resultant component values from mecahnical model that is used to predict the mechanism behind the asymmetric behavior of RAs.

Reactance	Resistance					
$Im\{Z\}$	$Re\{Z_0\}$	$Re\{Z_1\}$	$Re\{Z_2\}$	k_{01}	k_{21}	
0.917	0.484	1.252	1.899	4.201	6.908	Ns/m

5. DISCUSSION

5.1 Effect of Stimulus Location on RA Response

The spread of mechanical stimulation through the glabrous skin in proximal and distal direction was studied by stimulating afferents in distal and proximal locations, respectively, whereas the RF center was the middle point between these locations.

The mean absolute spike threshold and entrainment threshold for proximal stimulation of RAs were observed to be significantly higher than those for distal stimulations. Higher thresholds for proximal stimulation (Figure 5.1) indicated that the spread of mechanical stimulus in distal direction was worse than that in proximal direction.

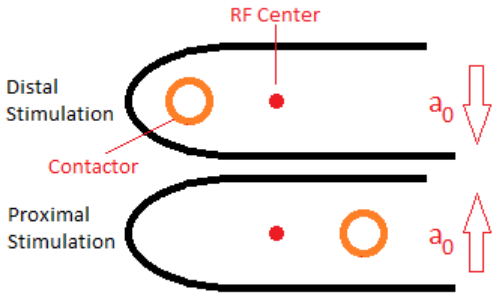

Figure 5.1 Diagram showing the change of a_0 relative to stimulation point.

Previous studies showed that the innervation density of mechanoreceptive fibers is higher distally [17, 18, 19]. Therefore, the psychophysical thresholds were expected to be lower distally. But in the study of Güçlü and Bolanowski (2005), this was not the case; psychophysical thresholds for non-Pacinian channel (NP) I mediated by RAs were nearly constant along the proximo-distal axis of the phalanx [1]. That could be explained by either a uniform distribution of mechanorecetors along the skin or nonuniform spread of mechanical disturbance through the skin. The theory of uniform distribution of mechanoreceptors along the skin is not congruent with the findings of histological and electrophysiological studies. In addition, the results mentioned in previous paragraph supports the latter reasonable assumption and may accounted for the uniform psychophysical detection threshold for the finger [1, 60], because the better spread of mechanical stimulus in proximal direction may counterbalance the effects of

innervation density which is higher distally.

For instance, according to the results of this study, if the innervation density of mechanoreceptors was uniform, there would be more units activated proximally. However, because distal regions have higher innervation density than proximal regions, the activation would be nearly uniform in both direction causing a uniform psychophysical threshold on the skin.

In order to use this data for population modeling, additional psychophysical experiments should be done to validate the model such as psychophysical detection threshold profile of the human distal phalanx. Once such population model is constructed, it can be used, basically, together with force transducers to build a neuroprosthesis; For example, a matrix of force transducers would be adequate to localize the stimulus and determine its amplitude. Information gathered from this transducer matrix can be modulated with population model, and sent to somatosensory cortex as tactile feedback.

There would be two problems with such a system; first, The force transducer array should be thin and elastic enough not to avert the movements. Designing such a force transducer array that could be implemented or worn to related end organ (for instance hands or/and foot) might be difficult and costly. Second, managing the inputs from this array and processing them would cause time lags. Time lag would be dependent on the number of force transducers and the speed of system processor. The number of transducers in the array would depend on the area of target skin that would be covered and also its representation in the primary somatosensory cortex which also would determine the number of stimulation electrodes.

5.2 Effect of Contactor Size on RA Response

The spatial summation properties of individual mechanoreceptive fibers were studied by changing contactor size at different distances from RF center. Although increment of contactor size increased the mean absolute spike threshold and the mean entrainment threshold of RAs for RF center stimulation and decreased them for distant stimulations, these effects of contactor size were not statistically significant.

Goodwin et al. (1995) have studied the response profiles of SAIs and RAs in primates under sustained mechanical stimulus, and they found that responses of SAIs increased as the curvature of stimulation probe increased, whereas the responses of RAs were small and did not vary [12]. Also, Vega-Bermudez and Johnson (1999) tested SAIs and RAs in primates with multiple probe indentations and found that the increment of probe number reduced the response of these afferents [15]. The difference between the findings of the literature mentioned above and my study may be due to different animals and stimulus conditions that were used. In addition, the smallest contactor available in this study was larger than those used in literature mentioned above, relative to the finger width of the subject. If much smaller contactor sizes were available, there might be significant differences between the smallest and the largest contactor sizes. However, because of technical difficulty, it was not possible to obtain smaller plastic contactors, and the metal contactors that could be smaller might have caused permanent damage to the rat glabrous skin during stimulation.

5.3 Skin Mechanics and RA Response

Mechanical impedance of the skin was found to be nonuniform through the skin. This finding is in agreement with the findings of Güçlü and Bolanowski (2005) [1]. However, in the study presented here, the impedance of skin was found to be governed by the resistance whereas the impedance measurements of Güçlü and Bolanowski (2005) [1] was governed by the stiffness reactance of the skin. The difference between these two findings is probably due to the size of the contactor relative to the finger size and the different subject species.

A more resistive skin in proximal regions is consistent with the higher mean threshold value for proximal stimulations such that energy of mechanical stimulus is dissipated at where it is applied before it spreads in distal direction. Likewise, the mechanical stimulus applied to distal locations where the resistance is small will have more energy to spread in proximal direction.

Another possible explanation for the asymmetric response profile of RAs may be the mechanical model presented above. This model suggests horizontal spring com-

ponents representing the stiffness of the surface of the skin. According to this model, the spring in proximal direction has a higher stiffness than the other spring in distal direction, so that a given constant indentation at distal locations would cause higher stress, therefore strain at proximal locations. This mechanical model may pave the way for the modification of RA population models in order to predict psychophysical thresholds for tactile sensation.

In addition, the model can be used to produce more realistic artificial skin structures. Such a elastic material shall have anisotropic mechanical properties. Behavior of the skin would be dependent on the direction of force. Furthermore, such an elastic material can be covered on transducers which will emulate the mechanoreceptors, so that it would attenuate mechanical vibrations spreading in one direction with a coefficient greater than one for the other direction. Such a mechanical filter system would provide a more realistic input for the cortical stimulation system.

5.4 Future Work

The data presented here can be used for population modeling, but additional psychophysical experiments, such as determining the psychophysical detection threshold profile of human distal phalanx, are necessary. With a successive population model direction selective tactile transducer can be designed.

To get further knowledge about how the peripheral input is processed in cortex, cortical sub-modality maps will be studied in primary somatosensory cortex hind limb region of anesthetized and alert rats, and spatial properties of cortical neurons in S I cortex and possible inputs from different types of tactile afferents onto these neurons will be studied. That will give the information of how to use peripheral population model for the cortical stimulation which will emulate the sensation of touch. Furthermore, improvement of population models for cortical neurons will be possible.

The data gathered from experiments mentioned above may be used to design of neuroprosthesis.

APPENDIX A. Mechanical Model of The Skin: Mathematical and Computational Background

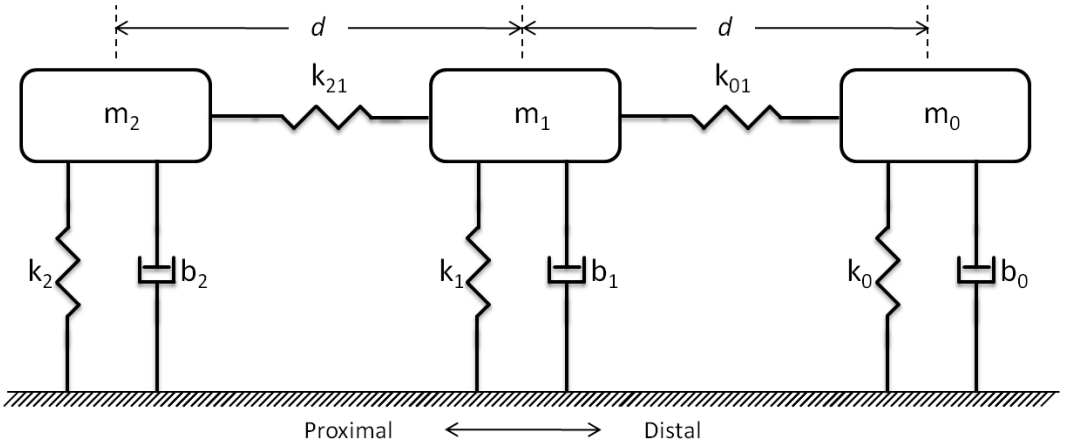

Figure A.1 Mechanical model used to solve possible mechanisms behind the mechanical stimulus spread through the skin.

For model shown in Figure A.1 following calculations were done:

$$F_0 = v_0 Z_0 + k_{01} f(l_0, l_1) \quad \text{(A.1)}$$

$$F_1 = v_1 Z_2 + k_{01} f(l_1, l_0) + k_{21} f(l_1, l_2) \quad \text{(A.2)}$$

$$F_2 = v_2 Z_2 + k_{21} f(l_2, l_1) \quad \text{(A.3)}$$

Assume that v, Z and spring displacement functions (f) have real and imaginary components, but F has only real component;

$$F_0 = (v_0 Cos\phi_0 + j v_0 Sin\phi_0)(b_0 + jI_0) + k_{01} f(l_0, l_1) \quad \text{(A.4)}$$

$$= (v_0 b_0 Cos\phi_0 - v_0 I_0 Sin\phi_0) + j(v_0 I_0 Cos\phi_0 + v_0 b_0 Sin\phi_0) + k_{01} f(l_0, l_1) \quad \text{(A.5)}$$

Impedance measurements showed that the impedance is governed by the resistance of the skin, and reactance showed relatively small variation along proximo-distal axis (for detailed information see Section 4.3.1). To simplify the system, reactance of the skin (I_i) was assumed to be uniform ($I_i = I$). Therefore, there is a system of

equations with 6 unknowns (I, b_0, b_1, b_2, k_{01}, k_{21}) and 6 equations.

$$F_0 - v_0 b_0 Cos\phi_0 + v_0 I Sin\phi_0 - k_{01} Re\{f(l_0, l_1)\} = 0 \quad \text{(A.6)}$$

$$v_0 I Cos\phi_0 + v_0 b_0 Sin\phi_0 + k_{01} Im\{f(l_0, l_1)\} = 0 \quad \text{(A.7)}$$

$$F_1 - v_1 b_1 Cos\phi_1 + v_1 I Sin\phi_1 - k_{01} Re\{f(l_1, l_0)\} - k_{21} Re\{f(l_1, l_2)\} = 0 \quad \text{(A.8)}$$

$$v_1 I Cos\phi_1 + v_1 b_1 Sin\phi_1 + k_{01} Im\{f(l_1, l_0)\} + k_{21} Im\{f(l_1, l_2)\} = 0 \quad \text{(A.9)}$$

$$F_2 - v_2 b_2 Cos\phi_2 + v_2 I Sin\phi_2 - k_{21} Re\{f(l_2, l_1)\} = 0 \quad \text{(A.10)}$$

$$v_2 I Cos\phi_2 + v_2 b_2 Sin\phi_2 + k_{21} Im\{f(l_2, l_1)\} = 0 \quad \text{(A.11)}$$

where displacement functions were estimated as the following:

While stimulating at m_0;

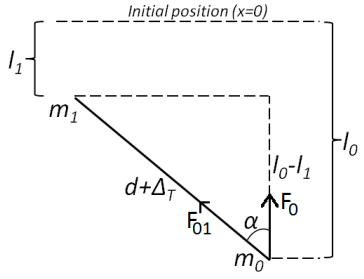

Figure A.2 Indentation at m_0 and resultant displacement at m_1.

In Figure A.2, F_0 is the force due to the force reflected by point impedance components and vertical component of tangential stretch force (F_{01}) where;

$$F_{01} = k_{01}\Delta_T \quad \text{(A.12)}$$

$$F'_{01} = k_{01}\Delta_T Cos\alpha \quad \text{(A.13)}$$

In Eq. A.13 Δ_T is the amount of stretch of skin surface, and $Cos\alpha$ is used so that vertical component of F_{01} could be estimated. Because it is not possible to estimate Δ_T and α without doing additional complex experiments, a function that will

estimate the amount of vertical stretch of skin surface with known values; v, ϕ and d.

$$l_0 = s_0 + x_0, \quad l_1 = s_1 + x_1,$$

$$d^2 + (l_0 - l_1)^2 = d^2 + 2d\Delta_T + \Delta_T^2 \tag{A.14}$$

$$\Delta_T^2 << 2d\Delta_T \quad \rightarrow \quad \Delta_T = \frac{(l_0 - l_1)^2}{2d} \tag{A.15}$$

$$Cos\alpha = \frac{l_0 - l_1}{d + \Delta_T} = \frac{2d(l_0 - l_1)}{2d^2 + (l_0 - l_1)^2} \tag{A.16}$$

$$\Delta_T Cos\alpha = \frac{(l_0 - l_1)^3}{2d^2 + (l_0 - l_1)^2} \tag{A.17}$$

$$(l_0 - l_1)^2 << 2d^2 \quad \rightarrow \quad f(l_0, l_1) = \Delta_T Cos\alpha = \frac{(l_0 - l_1)3}{2d^2} \tag{A.18}$$

Linearization at s_0 and s_1;

$$f(l_0, l_1) \approx f(s_0, s_1) + \frac{\partial f(l_0, l_1)}{\partial l_0}|_{s_0,s_1}(l_0 - s_0) + \frac{\partial f(l_0, l_1)}{\partial l_1}|_{s_0,s_1}(l_1 - s_1) \tag{A.19}$$

$$f(l_0, l_1) = \frac{(s_0 - s_1)^3}{2d^2} + \frac{3(s_0 - s_1)^2}{2d^2}x_0 - \frac{3(s_0 - s_1)^2}{2d^2}x_1 \tag{A.20}$$

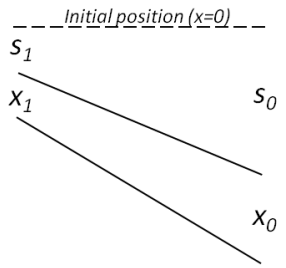

Figure A.3 Relation between pre-indentation (s_0), stimulus amplitude (x_0) and resultant displacements (s_1, x_1).

Assume that;

$$\frac{s_1}{s_0} \approx \frac{s_1 + x_1}{s_0 + x_0} \quad \rightarrow \quad s_1 = s_0 \frac{x_1}{x_0} \tag{A.21}$$

$$\begin{aligned} f(l_0, l_1) &= \frac{s_0^3}{2d^2}(1 - \frac{x_1}{x_0})^3 + \frac{3s_0^2}{2d^2}(1 - \frac{x_1}{x_0})^2(x_0 - x_1) && \text{(A.22)} \\ &= \frac{s_0^3}{2d^2}(1 - \frac{v_1/jw}{v_0/jw})^3 + \frac{3s_0^2}{2d^2}(1 - \frac{v_1/jw}{v_0/jw})^2(v_0/jw - v_1/jw) && \text{(A.23)} \\ &= \frac{s_0^3}{2d^2}(1 - \frac{v_1}{v_0})^3 + \frac{3s_0^2}{j2d^2w}(1 - \frac{v_1}{v_0})^2(v_0 - v_1) && \text{(A.24)} \\ &= \frac{s_0^3}{2d^2}(1 - \frac{v_1}{v_0})^3 - j\frac{3s_0^2}{2d^2w}(1 - \frac{v_1}{v_0})^2(v_0 - v_1) && \text{(A.25)} \end{aligned}$$

v_i is a complex number;

$$v_i = |v_i|e^{j(wt+\phi_i)} \tag{A.26}$$

Implement Eq. A.26 into Eq. A.24;

$$f(l_0, l_1) = \frac{s_0^3}{2d^2}(1 - \frac{|v_1|}{|v_0|}e^{j(\phi_1 - \phi_0)})^3 - j\frac{3s_0^2}{2d^2w}(1 - \frac{|v_1|}{|v_0|}e^{j(\phi_1 - \phi_0)^2}(|v_0|e^{j(wt+\phi_0)} - |v_1|e^{j(wt+\phi_1)}) \tag{A.27}$$

Justification for $\phi_0 \approx \phi_1$;

$$f(l_0, l_1) = \frac{s_0^3}{2d^2}(1 - \frac{|v_1|}{|v_0|})^3 - j\frac{3s_0^2}{2d^2w}(1 - \frac{|v_1|}{|v_0|})^2[(|v_0| - |v_1|)Cos\phi_0 + j(|v_0| - |v_1|)Sin\phi_0] \tag{A.28}$$

$$f(l_0, l_1) = \frac{s_0^3}{2d^2}(1 - \frac{|v_1|}{|v_0|})^3 + \frac{3s_0^2}{2d^2w}(1 - \frac{|v_1|}{|v_0|})^2(|v_0| - |v_1|)Sin\phi_0 - j\frac{3s_0^2}{2d^2w}(1 - \frac{|v_1|}{|v_0|})^2(|v_0| - |v_1|)Cos\phi_0 \tag{A.29}$$

When calculated in the same manner;

$$f(l_1, l_0) = -f(l_0, l_1) \tag{A.30}$$

$$f(l_1, l_2) = -f(l_2, l_1) \tag{A.31}$$

APPENDIX B. Mechanical Model of The Skin: Matlab Code to Solve The System of Equations for Mechanical Model

```
%%%%%%%%%%%%%%%%%%%%%%%%%%%%%%%%%%%%%%%%%%%%%%%%%%%%
%       Mechanical Components Solution Function      %
%                        05.07.2011                  %
%                      Master's Thesis               %
%                     İsmail Devecioğlu              %
%                                                    %
% 6 equations and 6 unkonw as following;             %
%        I, Reactance was assumed to be constant     %
%        b0,b1,b2, Resistances of diff. locations    %
%        k01, Horizontal spring in distal direction  %
%        k21, Horizontal spring in proxi direction   %
%                                                    %
%%%%%%%%%%%%%%%%%%%%%%%%%%%%%%%%%%%%%%%%%%%%%%%%%%%%
function [X,flag] = MechanicModel3(options)
    [X, ~, flag]= fsolve(@Fun,[0 0 0 0 0 0],options);
end

function F = Fun(x)% x = [I b0 b1 b2 k01 k21]
    % 0 : Distal, 1 : Middle, 2 : Proximal
    % Peak F and v values were converted into N and m/s, respectively
    % Divide by 2 for peak values and, divide by 10 V/N or V/ms-1
    F0 = 0.03008/20;  v0 = 0.04512/20;  fi0 = deg2rad(180-225.792);
    F1 = 0.07072/20;  v1 = 0.03936/20;  fi1 = deg2rad(180-220.032);
    F2 = 0.09840/20;  v2 = 0.03840/20;  fi2 = deg2rad(180-213.120);
    s0 = 0.0005;   s1 = 0.0005;   s2 = 0.0005;

    d = 0.001;
    freq = 40;
    w = 2*pi*freq;

    proxi = 102.399; cntr = 41.323; distal = 53.285;
```

```
32      rp = cntr/distal; rd = cntr/proxi;  %proximal and distal spread ...
           ratios, respectively
33
34      F = [F0-v0*x(2)*cos(fi0)+v0*x(1)*sin(fi0) - ...
           s0^3*x(5)*(1-rp)^3/(2*d^2) - ...
           3*s0^2*x(5)*(1-rp)^2*(v0-v0*rp)*sin(fi0)/(2*d^2*w);
35          v0*x(1)*cos(fi0)+v0*x(2)*sin(fi0) + ...
               3*s0^2*x(5)*(1-rp)^2*(v0-v0*rp)*cos(fi0)/(2*d^2*w);
36          F1-v1*x(3)*cos(fi1)+v1*x(1)*sin(fi1) - ...
               s1^3*x(6)*(1-rp)^3/(2*d^2) - ...
               3*s1^2*x(6)*(1-rp)^2*(v1-v1*rp)*sin(fi1)/(2*d^2*w) - ...
               s1^3*x(5)*(1-rd)^3/(2*d^2) - ...
               3*s1^2*x(5)*(1-rd)^2*(v1-v1*rd)*sin(fi1)/(2*d^2*w);
37          v1*x(1)*cos(fi1)+v1*x(3)*sin(fi1) + ...
               3*s1^2*x(6)*(1-rp)^2*(v1-v1*rp)*cos(fi1)/(2*d^2*w) + ...
               3*s1^2*x(5)*(1-rd)^2*(v1-v1*rd)*cos(fi1)/(2*d^2*w)
38          F2-v2*x(4)*cos(fi2)+v2*x(1)*sin(fi2) - ...
               s2^3*x(6)*(1-rd)^3/(2*d^2) - ...
               3*s2^2*x(6)*(1-rd)^2*(v2-v2*rd)*sin(fi2)/(2*d^2*w);
39          v2*x(1)*cos(fi2)+v2*x(4)*sin(fi2) + ...
               3*s2^2*x(6)*(1-rd)^2*(v2-v2*rd)*cos(fi2)/(2*d^2*w)];
40  end
```

REFERENCES

1. Guclu, B., and S. J. Bolanowski, "Vibrotactile thresholds of the non-pacinian i channel: Ii. predicting the effects of contactor location on the phalanx.," *Somatosensory and Motor Research*, Vol. 22, pp. 57–68, March/June 2005.

2. Andy, H. J., R. B. Stein, M. K. Haugland, T. Sinkjaer, W. K. Durfee, A. B. Schwartz, G. E. Loeb, and C. Kantor, "Neural signals for command control and feedback in functional neuromuscular stimulation: A review.," *J of Rehabilitation Research And Development*, Vol. 33, no. 2, pp. 145–157, 1996.

3. Fagg, A. F., N. G. Hatsopoulos, V. Lafuente, K. A. Moxon, S. Nemati, J. M. Rebesco, S. A. Solla, J. Reimer, D. Tkach, E. A. Pohlmeyer, and L. E. Miller, "Biomimetic brain machine interfaces for the control of movement.," *The Journal of Neuroscience*, Vol. 27, no. 44, pp. 11842–11846, 2007.

4. Haugland, M., and T. Sinkjaer, "Interfacing the body's own sensing receptors into neural prosthesis devices.," *Technology and Health Care*, Vol. 7, pp. 393–399, 1999.

5. Moritz, C. T., S. I. Perlmutter, and E. E. Fetz, "Direct control of paralysed muscles by cortical neurons.," *Nature*, Vol. 456, pp. 639–643, 2008.

6. Peckham, P. H., M. W. Keith, and A. A. Freehafer, "Restoration of functional control by electrical stimulation in the upper extremity of the quadriplegic patient.," *J Bone Joint Surg Am.*, Vol. 70, pp. 144–148, 1988.

7. Popovic, D. B., R. B. Stein, K. L. Jovanovic, A. Kostov, and W. W. Armstrong, "Sensory nerve recording for closed-loop control to restore motor functions.," *IEEE Transactions on Biomedical Engineering*, Vol. 40, no. 10, pp. 1024–1031, 1993.

8. Sinkjaer, T., M. Hansen, B. Upshaw, M. Haugland, and A. Kostov, "Processing sensory nerve signals meant for control of paralyzed muscles.," *IEEE Nordic Signal Processing Symposium*, June 1998.

9. Sinkjaer, T., M. Haugland, and J. Haase, "Natural neural sensing and artificial muscle control in man.," *Exp Brain Res.*, Vol. 98, no. 3, pp. 542–545, 1994.

10. London, B. M., L. R. Jordan, C. R. Jackson, and L. E. Miller, "Electrical stimulation of the proprioceptive cortex (area 3a) used to instruct a behaving monkey.," *IEEE Transactions on Neural Systems and Rehabilitation Engineering*, Vol. 16, no. 1, pp. 32–36, 2008.

11. Romo, R., A. Hernandez, A. Zainos, and E. Salinas, "Somatosensory discrimination based on cortical microstimulation.," *Nature*, Vol. 392, pp. 387–390, 1998.

12. Goodwin, A. W., A. S. Browning, and H. E. Wheat, "Representation of curved surfaces in responses of mechanoreceptive afferent fibers innervating the monkey's fingerpad.," *The Journal of Neuroscience*, Vol. 15(1), pp. 798–810, 1995.

13. Goodwin, A. W., V. G. Macefield, and J. W. Bisley, "Encoding of object curvature by tactile afferents from human fingers.," *Journal of Neurophysiology*, Vol. 78, pp. 2881–2888, 1997.

14. Vega-Bermudez, F., and K. O. Johnson, "Sa i and ra receptive fields, response variability, and population responses mapped with a probe array.," *Journal of Neurophysiology*, Vol. 81, pp. 2701–2710, 1999.

15. Vega-Bermudez, F., and K. O. Johnson, "Surround suppression in the responses of primate sa1 and ra mechanoreceptive afferents mapped with a probe array.," *Journal of Neurophysiology*, Vol. 81, pp. 2711–2719, 1999.

16. Ray, R. H., and G. S. Doetsch, "Coding of stimulus location and intensity in populations of mechanosensitive nerve fibers of the racoon: I. single fiber response properties.," *Brain Research Bulletin*, Vol. 25, pp. 517–532, 1990.

17. Johansson, R. S., and A. B. Vallbo, "Tactile sensibility in the human hand: relative and absolute densities of four types of mechanoreceptive units in glabrous skin.," *Journal of Physiology*, Vol. 286, pp. 283–300, 1979.

18. Vallbo, A. B., and R. S. Johansson, "The tactile sensory innervation of the glabrous skin of the human hand," in *Active Touch, the Mechanism of Recognition of Objects by Manipulation* (Gordon, G., ed.), pp. 29–54, Oxford, UK: Pergamon Press Ltd, 1978.

19. Darian-Smith, I., and P. Kenins, "Innervation density of mechanoreceptive fibres supplying glabrous skin of the monkey's index finger.," *Journal of Physiology*, Vol. 309, pp. 147–155, 1980.

20. Gardner, E. P., and J. H. Martin, "Coding of sensory information," in *Principle of Neural Science 4th ed.*, pp. 411–429, New York, USA: McGraw-Hill, 2000.

21. Hendry, S. H., S. S. Hsiao, and M. C. Brown, "Fundamentals of sensory systems," in *Fundamental Neuroscience*, pp. 535–548, Burlington, USA: Academic Press, 2008.

22. McGrath, J. A., and J. Uitto, "Anatomy and organization of human skin," in *Rook's Textbook of Dermatology* (Burns, T., S. Breathnach, N. Cox, and C. Griffiths, eds.), pp. 3.1–3.53, West Sussex, UK: Wiley-Blackwell, 2010.

23. Gardner, E. P., J. H. Martin, and T. M. Jessell, "The bodily senses," in *Principle of Neural Science 4th ed.*, pp. 430–449, New York, USA: McGraw-Hill, 2000.

24. Iggo, A., and D. W. Young, "Cutaneous thermoreceptors and thermal nociceptors.," in *The Somatosensory System*, pp. 5–22, Stuttgart, Germany: Thieme, 1975.

25. Iggo, A., "Somatosensory system," in *Handbook of Sensory Physiology*, Berlin, Germany: Springer-Verlag, 1973.

26. Iggo, A., "Cutaneous receptors," in *The Peripheral Nervous System*, pp. 347–404, New York, USA: Plenum, 1974.

27. Metz, D., and T. Luger, "Nervous system in the skin.," in *The Biology of the Skin*, pp. 153–176, New York, USA: Parthenon, 2000.

28. Lynn, B., "Cutaneous sensation.," in *Physiology, Biochemistry and Molecular Biology of the Skin*, pp. 779–815, New York, USA: Oxford University Press, 1991.

29. Bolanowski, S., "Somatosensory coding," in *Signals and Perception: The Fundamentals of Human Sensation*, New York, USA: Palgrave Macmillan, 2002.

30. Archer, C. B., "Functions of the skin," in *Rook's Textbook of Dermatology* (Burns, T., S. Breathnach, N. Cox, and C. Griffiths, eds.), pp. 4.1–4.11, West Sussex, UK: Wiley-Blackwell, 2010.

31. Ridley, A., "Silver staining of nerve endings in human digital glabrous skin.," *Journal of anatomy*, Vol. 104, no. 1, pp. 41–48, 1969.

32. Leem, J. W., W. D. Willis, and J. M. Chung, "Cutaneous sensory receptors in the rat foot.," *Journal of Neurophysiology*, Vol. 69, pp. 1684–1699, 1993.

33. Bolanowski, S. J., and J. J. Zwislocki, "Intensity and frequency characteristics of pacinian corpuscles. i. action potentials.," *Journal of Neurophysiology*, Vol. 51, no. 4, pp. 793–810, 1984.

34. Bolanowski, S. J., and J. J. Zwislocki, "Intensity and frequency characteristics of pacinian corpuscles. ii. receptor potentials.," *Journal of Neurophysiology*, Vol. 51, no. 4, pp. 812–830, 1984.

35. Johnson, K. O., "The roles and functions of cutaneous mechanoreceptors.," *Current Opinion in Neurobiology*, Vol. 11, pp. 455–461, 2001.

36. Hendry, S., and S. Hsiao, "Somatosensory system," in *Fundamental Neuroscience*, pp. 581–608, Burlington, USA: Academic Press, 2008.

37. Press, D., S. Mutlu, and B. Guclu, "Evidence of fast serotonin transmission in frog slowly adapting type i responses.," *Somatosensory and Motor Research*, Vol. 27, no. 4, pp. 174–185, 2010.

38. Iggo, A., and A. R. Muir, "The structure and function of a slowly adapting touch corpuscle in hairy skin.," *Journal of Physiology*, Vol. 200, no. 3, pp. 763–796, 1969.

39. Leem, J. W., W. D. Willis, S. C. Weller, and J. M. Chung, "Differential activation and classification of cutaneous afferents in the rat.," *Journal of Neurophysiology*, Vol. 70, pp. 2411–2424, 1993.

40. Johansson, R. S., U. Landstrom, and R. Lundstrom, "Responses of mechanoreceptive afferent units in the glabrous skin of the human hand to sinusoidal skin displacements.," *Brain Research*, Vol. 244, pp. 17–25, 1982.

41. Darian-Smith, I., "The sense of touch: Performance and peripheral neural processes.," *Comprehensive Physiology*, pp. 739–788, 2011.

42. Pawson, L., L. T. Prestia, G. K. Mahoney, B. Guclu, P. J. Cox, and A. K. Pack, "Gabaergic/glutamatergic-glial/neuronal interaction contributes to rapid adaptation in pacinian corpuscles.," *The Journal of Neuroscience*, Vol. 29, 2009.

43. Pease, D. C., and T. A. Quilliam, "Electron microscopy of the pacinian corpuscle.," *J. Biophysic. and Biochem. Cytol.*, Vol. 3, no. 3, pp. 109–116, 1957.

44. Johnson, K. O., T. Yoshioka, and F. Vega-Bermudez, "Tactile functions of mechanoreceptive afferents innervating the hand.," *Journal of Clinical Neurophysiology*, Vol. 17, no. 6, pp. 539–558, 2000.

45. Pearson, K., and J. Gordon, "Spinal reflexes," in *Principle of Neural Science 4th ed.*, pp. 713–736, New York, USA: McGraw-Hill, 2000.

46. Martin, J. H., "Spinal somatic sensory systems," in *Neuroanatomy: text and atlas, 3rd Ed.*, pp. 107–133, USA: McGraw-Hill, 2003.

47. Wang, Q., and V. Hayward, "In vivo biomechanics of the fingerpad skin under local tangential traction.," *Journal of Biomechanics*, Vol. 40, pp. 851–860, 2007.

48. Schultz, G. S., G. Ladwig, and A. Wysocki, "Extracellular matrix: review of its roles in acute and chronic wounds.," *World Wide Wounds (Online Resourse)*, August 2005. http://www.worldwidewounds.com/2005/august/Schultz/Extrace-Matric-Acute-Chronic-Wounds.html, Last visit: June 2011.

49. Bischoff, J. E., E. M. Arruda, and K. Grosh, "Finite element modeling of human skin using an isotropic, nonlinear elastic constitutive model.," *Journal of Biomechanics*, Vol. 33, pp. 645–652, 2000.

50. Delalleau, A., G. Josse, J. M. Lagarde, H. Zahouani, and J. M. Bergheau, "A nonlinear elastic behavior to identify the mechanical parameters of human skin in vivo.," *Skin Research and Technology*, Vol. 14, pp. 152–164, 2008.

51. Evans, S. L., and C. A. Holt, "Measuring the mechanical properties of human skin in vivo using digital image correlation and finite element modelling.," *Journal of Strain Analysis*, Vol. 44, pp. 337–345, 2009.

52. Khatyr, F., C. Imberdis, P. Vescovo, D. Varchon, and J. M. Lagarde, "Model of the viscoelastic behaviour of skin in vivo and study of anisotropy.," *Skin Research and Technology*, Vol. 10, pp. 96–103, 2004.

53. Lokshin, O., and Y. Lanir, "Viscoelasticity and preconditioning of rat skin under uniaxial stretch: Microstructural constitutive characterization.," *Journal of Biomechanical Engineering*, Vol. 131(3):031009, 2009.

54. Molinari, E., M. Fato, G. de Leo, D. Riccardo, and F. Beltrame, "Simulation of the biomechanical behavior of the skin in virtual surgical applications by finite element method.," *IEEE Transactions on Biomedical Engineering*, Vol. 52, no. 9, pp. 1514–1521, 2005.

55. Wu, J. Z., R. G. Dong, W. P. Smutz, and A. W. Schopper, "Nonlinear and viscoelastic characteristics of skin under compression: experiment and analysis.," *Bio-Medical Materials and Engineering*, Vol. 13, pp. 373–385, 2003.

56. Standring, S., *Gray's Anatomy: The Anatomical Basis of Clinical Practice 40th Edition*, Spain: Elsevier Limited, 2008.

57. Moore, T. J., "A survey of the mechanical characteristics of skin and tissue in response to vibratory stimulation.," *IEEE Transactions on Man-Machine Systems*, Vol. MMS-11, no. 1, pp. 79–84, 1970.

58. Cohen, J. C., J. C. Makous, and S. J. Bolanowski, "Under which conditions do the skin and probe decouple during sinusoidal vibrations?," *Exp Brain Res*, Vol. 129, pp. 211–217, 1999.

59. Gok, C., I. Devecioglu, and B. Guclu, "Relationship between the structure of epidermis and mechanical properties of rat glabrous skin.," *Unpublished conference paper.*, 2011.

60. Gescheider, G. A., S. J. Bolanowski, J. V. Pope, and R. T. Verillo, "A four-channel analysis of the tactile sensitivity of the fingertip: frequency selectivity, spatial summation, and temporal summation.," *Somatosensory and Motor Research*, Vol. 19, no. 2, pp. 114–124, 2002.